AD-A121 702 SIMULATION OF ACTIVE AND PASSIVE MILLIMETER-WAVE (35GHZ) SENSORS BY TIME..(U) ARMY ARMAMENT RESEARCH AND DEVELOPMENT COMMAND ABERDEEN PROVI..

UNCLASSIFIED D F STRENZWILK ET AL. NOV 82 ARBRL-MR-03214 F/G 17/2 NL

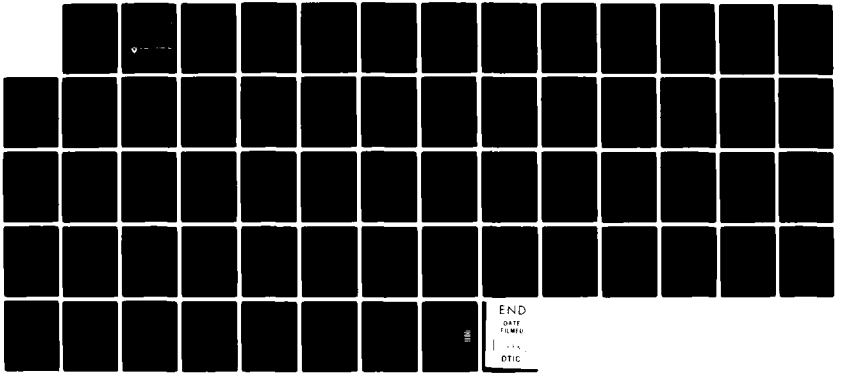

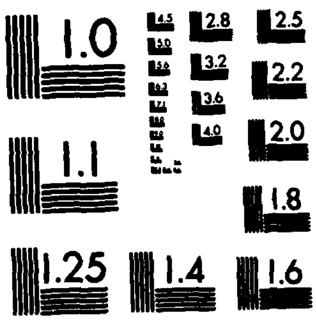

MICROCOPY RESOLUTION TEST CHART
NATIONAL BUREAU OF STANDARDS-1963-A

AD

MEMORANDUM REPORT ARBRL-MR-03214

SIMULATION OF ACTIVE AND PASSIVE MILLIMETER-WAVE (35GHz) SENSORS BY TIME SERIES ANALYSIS

Denis F. Strenzwilk
Richard T. Maruyama

November 1982

US ARMY ARMAMENT RESEARCH AND DEVELOPMENT COMMAND
BALLISTIC RESEARCH LABORATORY
ABERDEEN PROVING GROUND, MARYLAND

Destroy this report when it is no longer needed.
Do not return it to the originator.

Secondary distribution of this report is prohibited.

Additional copies of this report may be obtained from the National Technical Information Service, U. S. Department of Commerce, Springfield, Virginia 22161.

The findings in this report are not to be construed as an official Department of the Army position, unless so designated by other authorized documents.

The use of trade names or manufacturers' names in this report does not constitute indorsement of any commercial product.

UNCLASSIFIED

SECURITY CLASSIFICATION OF THIS PAGE *(When Data Entered)*

REPORT DOCUMENTATION PAGE	READ INSTRUCTIONS BEFORE COMPLETING FORM
1. REPORT NUMBER: MEMORANDUM REPORT ARBRL-MR-03214	2. GOVT ACCESSION NO.: AD A121702
3. RECIPIENT'S CATALOG NUMBER	
4. TITLE *(and Subtitle)*: Simulation of Active and Passive Millimeter-Wave (35GHz) Sensors by Time Series Analysis	5. TYPE OF REPORT & PERIOD COVERED
	6. PERFORMING ORG. REPORT NUMBER
7. AUTHOR(s): Denis F. Strenzwilk Richard T. Maruyama	8. CONTRACT OR GRANT NUMBER(s)
9. PERFORMING ORGANIZATION NAME AND ADDRESS: US Army Ballistic Research Laboratory ATTN: DRDAR-BLB Aberdeen Proving Ground, MD 21005	10. PROGRAM ELEMENT, PROJECT, TASK AREA & WORK UNIT NUMBERS: RDT&E 1L162618AH80
11. CONTROLLING OFFICE NAME AND ADDRESS: US Army Armament Research & Development Command US Army Ballistic Research Laboratory (DRDAR-BL) Aberdeen Proving Ground, MD 21005	12. REPORT DATE: November 1982 13. NUMBER OF PAGES: 60
14. MONITORING AGENCY NAME & ADDRESS *(if different from Controlling Office)*	15. SECURITY CLASS. *(of this report)*: UNCLASSIFIED 15a. DECLASSIFICATION/DOWNGRADING SCHEDULE

16. DISTRIBUTION STATEMENT *(of this Report)*

Approved for public release; distribution unlimited.

17. DISTRIBUTION STATEMENT *(of the abstract entered in Block 20, if different from Report)*

18. SUPPLEMENTARY NOTES

19. KEY WORDS *(Continue on reverse side if necessary and identify by block number)*

Time Series Analysis, Radar, Radiometer, Clutter, Millimeter-Wave Sensors, Background Noise, Simulation

20. ABSTRACT *(Continue on reverse side if necessary and identify by block number)*

(hmn)

Analog voltage signals from a millimeter-wave (MMW) radiometer (passive sensor) and radar (active sensor) were collected over varying grassy terrains at Aberdeen Proving Ground (APG), Maryland in July 1980. These measurements were made as part of continuing studies of MMW sensors for smart munitions. The signals were digitized at a rate of 2,000 observations per second and then analyzed by the Box and Jenkins time series approach. This analysis reports on

DD FORM 1 JAN 73 1473 EDITION OF 1 NOV 65 IS OBSOLETE

UNCLASSIFIED

SECURITY CLASSIFICATION OF THIS PAGE *(When Data Entered)*

the characterization of these data sets. The passive time series signals resulted in a simple autoregressive-moving average process, similar to a previous set of data taken at Rome Air Development Center in Rome, N.Y. by Ballistic Research Laboratory. On the other hand, the radar data (active sensor) required a data transformation to enhance the analysis. In both cases the signals were well characterized using the Box-Jenkins time series approach.

TABLE OF CONTENTS

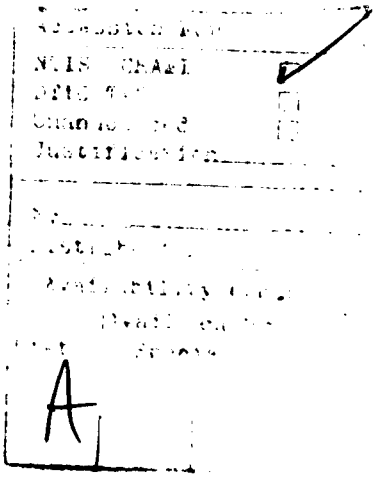

LIST OF FIGURES

LIST OF FIGURES (CONTINUED)

LIST OF TABLES

I. INTRODUCTION

The responses of a millimeter-wave (MMW) radiometric (passive) sensor and a MMW radar (active) sensor to varying grassy terrains and targets were measured in July 1980 by BRL at Aberdeen Proving Ground (APG),Maryland. These measurements were made as part of continuing studies of MMW sensors for smart munitions. The analog voltage signals of the sensors were digitized at a rate of 2,000 observations per second,which was the same rate as the data recorded in August 1978 at Rome , New York. Test ranges were selected on Spesutie Island at APG. Then a helicopter was instrumented with an active and passive sensor on a spinning mount,which revolved at three (3) revolutions per second (rps) and was flown over the ranges on runs of several seconds duration. The passive or radiometric sensor was similar to the sensor used in the August 1978 test and thus the results were expected to have similar characteristics (see Figure 1).

The analysis of passive and active sensors is an on-going investigation at BRL. By using the Box-Jenkins[1] time series modeling approach a successful simulation[2] of the response of the passive sensor to varying grassy terrains in the 1978 tests at Rome has provided a realistic way to introduce false alarms and the distortion of the target signatures due to clutter into the study of the performance of various weapon systems. The response of the passive sensor was modeled by an Autoregressive-Intergrated-Moving-Average (ARIMA) process, which was first order autoregressive and first order moving average. The purpose of this research was to provide a simulation of the response of the passive and active sensors used in the 1980 APG tests by time series analysis. The model for the passive sensor was expected to be the same as the previous study.

On the other hand, the signal response for the radar (active) sensor was different in character, in that the signal patterns were not symmetric about the mean. That is, the signals in the positive directions were larger than in the negative direction (see Figure 2). In order to best utilize the Box-Jenkins time series modeling approach, a data transformation was necessary. The purpose of the data transformation was to employ the data in a form that will improve the analysis, without altering the data structure (in terms of the autocorrelation and partial autocorrelation function).

One of the Biomedical computer packages (BMDP) from UCLA,viz., Statistical Software for Time Series Analysis, was used for this analysis[3]. There are two estimation methods of the model parameters,the first being the conditional least square method (LSM) and the second being the backcasting method (BM).

---

[1] Box,G. E. P. and Jenkins, G. M., "Time Series Analysis: Forecasting and Control",Holden-Day,Inc.,San Francisco,Ca.,1970.

[2] Maruyama,R. T.,"A Time Series and Intervention Analysis of Millimeter-Wave (MMW) Radiometric Data",ARBRL-TR-02338,July 1981.

[3] Lon-Mu Liu,"User's Manual for BMDQ2T(TSPACK) Time Series Analysis (Box-Jenkins)",Technical Report No. 57, Department of Biomathematics , UCLA, 1979.

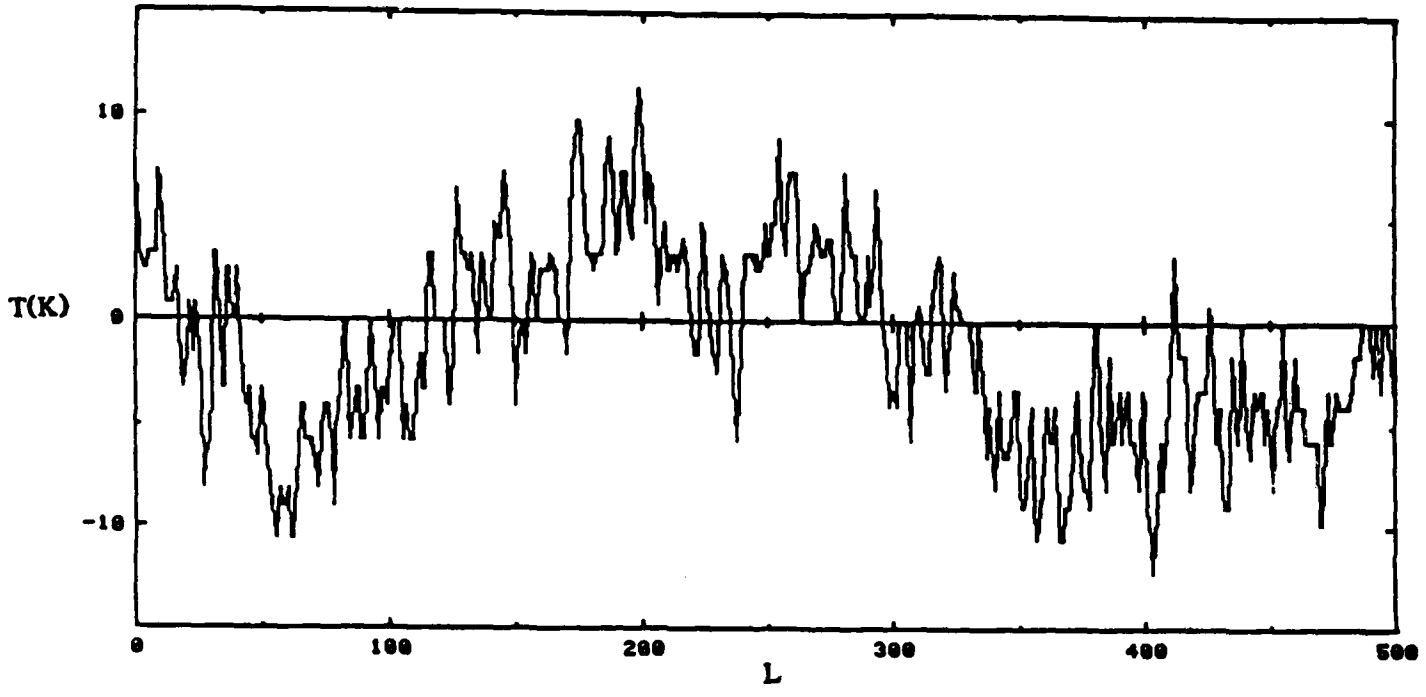

Figure 1. The actual contrast Temperature Data T(K) for a Field at 90m Slant Range is Plotted Against the Integer Number L of Time Steps, ($\Delta t = .5\ ms$).

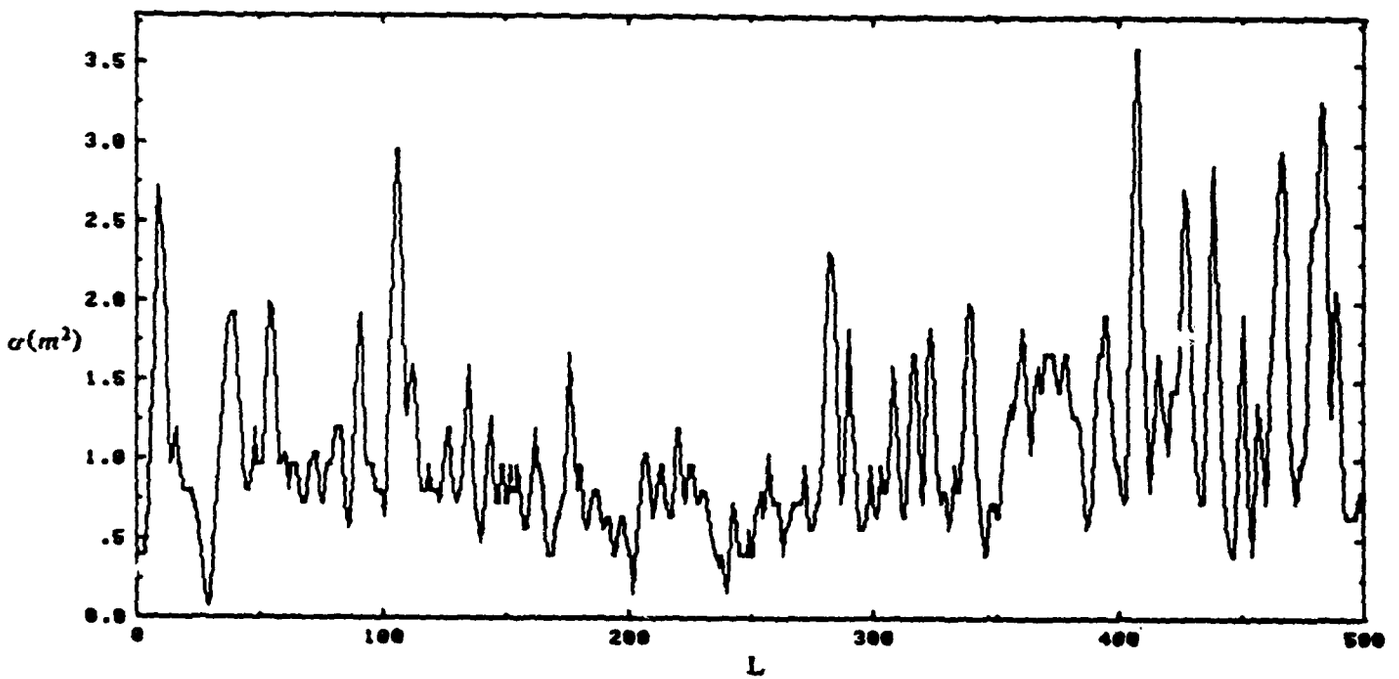

Figure 2. The Actual Radar Cross Section $\sigma(m^2)$ for a Field at 90m Slant Range is Plotted Against the Integer Number L of Time Steps, $(\Delta t = .5\ ms)$.

II. TIME SERIES ANALYSIS

In this report time series analysis is used to simulate the signals from a passive and an active (MMW) sensor. It seems fitting to explain the basic ideas of time series, and to introduce some terminology so that the reader can better follow our report. The digitized values of the analog voltage signals represent a time series $Z_1, Z_2, \ldots, Z_N$ of N successive observations, which are regarded as a sample realization from an infinite population of such time series that could have been generated by the stochastic process. Both the radiometer and radar data have been modeled as though they were derived from a **stationary** process, which implies that the mean and variance are constant, and that the error terms are normally distributed.

An **autoregressive model** is one in which the current value of the process is expressed as a finite, linear aggregrate of the previous values of the process and an error term or so-called shock $a_t \approx N(0,\sigma_a{}^2)$, where σ_a is the standard deviation of the white noise. If the data is **centered** about the mean μ, then $\tilde{Z}_t = Z_t - \mu$ can be represented as an autoregressive (AR) process of order p, viz.,

$$\tilde{Z}_t = \phi_1 \tilde{Z}_{t-1} + \phi_2 \tilde{Z}_{t-2} + \cdots + \phi_p \tilde{Z}_{t-p} + a_t \, . \tag{II.1}$$

The model contains p+2 unknown parameters $\mu, \phi_1, \phi_2, \ldots, \phi_p$, $\sigma_a{}^2$, which must be estimated from the data.

An **autoregressive operator** of order p can also be defined in terms of the **backward shift operator** B (where $BZ_t = Z_{t-1}$) by

$$\phi(B) = 1 - \phi_1 B - \phi_2 B^2 - \cdots - \phi_p B^p \, , \tag{II.2}$$

and then Equation (II.1) becomes

$$\phi(B)\tilde{Z}_t = a_t \, . \tag{II.3}$$

A **moving average** (MA) process of order q is one in which $\tilde{Z}_t$ is made to be linearly dependent on a finite number q of previous a's, viz.,

$$\tilde{Z}_t = a_t - \theta_1 a_{t-1} - \theta_2 a_{t-2} - \cdots - \theta_q a_{t-q} \, . \tag{II.4}$$

It contains q+2 unknown parameters $\mu, \theta_1, \ldots, \theta_q$, $\sigma_a{}^2$, which must be estimated from the data.

A **moving average operator** of order q can be defined by

$$\theta(B) = 1 - \theta_1 B - \theta_2 B^2 - \cdots - \theta_q B^q \, , \tag{II.5}$$

so that Equation (II.4) can be written as

$$\tilde{Z}_t = \theta(B)a_t \ . \qquad \text{(II.6)}$$

Frequently, the two processes are combined to include both autoregressive and moving average terms in the model. Thus, the **mixed autoregressive -moving average model** is

$$\tilde{Z}_t = \phi_1\tilde{Z}_{t-1} + \cdots + \phi_p\tilde{Z}_{t-p} + a_t - \theta_1 a_{t-1} - \cdots - \theta_q a_{t-q} \ , \qquad \text{(II.7)}$$

or

$$\phi(B)\tilde{Z}_t = \theta(B)a_t \ , \qquad \text{(II.8)}$$

where there are p+q+2 unknown parameters $\mu;\phi_1,...,\phi_p;\ \theta_1,...,\theta_q;\ \sigma_a^2$ that must be estimated from the data.

Many time series exhibit **nonstationary** behavior. Certain types of nonstationarity can be removed by differencing the data. In terms of the **backward shift operator** B, the time series observations (Z_t) can be differenced d times. Thus, the new operator $\Phi(B)$ can be defined as

$$\Phi(B) = \phi(B)(1-B)^d \ , \qquad \text{(II.9)}$$

where $\phi(B)$ is the stationary operator in Equation (II.2). The general model, which represents the homogeneous nonstationary behavior can now be written as

$$\Phi(B)Z_t = \phi(B)(1-B)^d Z_t = \theta(B)a_t \ , \qquad \text{(II.10)}$$

that is

$$\phi(B)W_t = \theta(B)a_t \ , \qquad \text{(II.11)}$$

where

$$W_t = (1-B)^d Z_t \ . \qquad \text{(II.12)}$$

It can be seen that Equation (II.11) means that the d'th difference of the process is stationary. In our report d was always zero since our original data was stationary. The process defined by Equation (II.11) and (II.12) is called an **autoregressive integrated moving average (ARIMA) process** of order (p,d,q).

Use was also made of the BMDQ2T(TSPACK) TIME SERIES PACKAGE computer program mentioned in reference 3. This program evaluates the **mean, standard deviation, autocorrelation function (ACF),** and the **partial autocorrelation function (PACF)** of the N successive observations of the Z_t's. A histogram of the variable Z and a cumulative histogram of the variable Z is also provided. When the radar data was analyzed the original data (Z_t) was transformed into (Y_t) by a natural log transformation (Box-Cox) and then all the above quantities were provided for the (Y_t).

The ACF is a diagnostic tool, which tells how the values of the time series, (Z_t, Z_{t-k}), separated by k time steps or k lags, are correlated with one another. The PACF is a diagnostic tool, which shows the autocorrelation between the values of the time series, (Z_t, Z_{t-k}), when the effects of the variables $Z_{t-1}, Z_{t-2}, \ldots, Z_{t-k+1}$ are fixed. If the ACF and PACF of the original data are plotted, a clue is given for a tentative starting ARIMA model. An AR process of order p has an ACF, which is infinite in extent with damped exponentials and/or damped sine waves, while its PACF is finite in extent and cuts off after p nonzero values. An MA process of order q has an ACF, which is finite in extent and cuts off after q nonzero values, while its PACF is infinite in extent and dominated by damped exponentials and/or sine waves. A mixed process of order (p,0,q) has an ACF, which is infinite in extent with damped exponentials and/or damped sine waves after the first q-p lags, while its PACF is infinite in extent and dominated by damped exponentials and/or sine waves after the first p-q lags.

After a tentative model has been identified, the ACF and PACF of the residuals (a_t), which are the estimates of the error terms for a particular sampling of data, are plotted to see if they indicate the normality or white noise assumed by the time series approach. The residuals of a white noise process have an ACF and PACF, which have value 1 at zero lag and value zero elsewhere. If the residuals do not appear to be normal, a new ARIMA (p,d,q) model is tried until the residuals indicate normality. The program also estimates the constants in the (p,d,q) model by the conditional least squares method and the backcasting method. For our problem the parameters found from the backcasting method were selected. There is only a slight difference in the values of the parameters evaluated by the different methods. The interested reader can find much more detail on time series analysis in reference 1.

III MILLIMETER-WAVE (MMW) RADIOMETRIC ANALYSIS

A previous set of data, which was taken over a grassy field under similar conditions at Rome, N.Y., in August 1978, was analyzed in 1981[2]. The spin rate of the radiometer at the Rome tests was 4 rps. The result of that investigation was that an ARIMA(1,0,1) process best described the passive signals. Because of the similarities in the sensors it was expected that a time series of the APG data would again result in a first order autoregressive-moving average (ARIMA(1,0,1)) process.

This analysis was done to characterize clutter data (background) free of any intervention such as, bodies of water,metallic vehicles,metal towers,etc. Both passive and active millimeter-wave signals were collected simultaneously. The sensors were mounted together such that the same section of terrain was being observed at the same instant of time. There is some difference in the area of the ground being observed by the two sensors. The footprint of the active sensor is smaller than that of the passive sensor.

The radiometric data shown in Figure 1 has been calibrated in Kelvins. The data that the following analysis concerns are uncalibrated. To obtain calibrated data the mean (6.43) of the uncalibrated data must be substracted from each uncalibrated data point and the result multiplied by a calbration constant of 81.4 K per unit.

The Autocorrelation Function (ACF) and Partial Autocorrelation Function (PACF) of all the data in this report were carried out to 36 lags on the BMDP package, but usually fewer lags were needed to display the important features. For the passive sensor the ACF and PACF are shown in Figure 3, and the values plotted are given in Table 1. The decaying characteristics of the ACF are theoretically associated with an AR(1) model. Thus, an ARIMA(1,0,0) model was first used to characterize this data.

The ARIMA(1,0,0) fit resulted in the residuals (a_t) of this fit having some remaining structure as shown in Figure 4. The values plotted are listed in Table 2. The ACF at lags one (1) and two (2) as well as the PACF at lags one and two have values that do not indicate normality. The lack of fit,determined from the analysis on the residuals, indicates that either a moving-average term or an autoregressive term should be added. The cutoff after the second PACF lag indicates that an autoregressive term should be added; hence an ARIMA(2,0,0) was attempted.

The ARIMA(2,0,0) model was fitted to the data set as shown in Figure 5. The values plotted are given in Table 3. The residual analysis of the ARIMA(2,0,0) model did remove the significant value of the ACF at lag one, but both values of the ACF and PACF at lag two (2) remain significant, indicating a need for further analysis. A histogram of the residuals in this case is shown in Figure 6, and gives questionable evidence of being normally distributed. The only unresolved problem area in the analysis of the ARIMA(2,0,0) was with the remaining residual autocorrelation at the second lag.

To resolve the problem of the significant value of the ACF at lag 2, a moving average term of order two was added to the ARIMA(2,0,0) structure. The ARIMA(2,0,(2)) fit, shown in Figure 7, did remove both the large values at lag 2 of the ACF and PACF to a point where it was adequate for the purpose of characterizing the data. The values are given in Table 4. Therefore, this time series analysis seemed satisfactory.

On the other hand, if a moving average term were added to the ARIMA(1,0,0) model instead of another autoregressive term, would the ARIMA(1,0,1) structure remove the remaining ACF lags? To answer this question the the ACF and PACF of the residuals were plotted in Figure 8, and their values are given in Table 5. A histogram of the residuals indicated normality as can be seen in Figure 9. The only negative indication is that the ACF at lag two (2) and the PACF past lag two indicated a decaying effect.

The analysis of these residuals indicated that an additional moving average term might be included to remove the autocorrelation (ACF) at lag two;hence, the ARIMA(1,0,2) model was the next logical step in the sequence of analysis for the millimeter-wave radiometric data. The plot of the residuals shown in Figure 10 again indicated some minor problems with the analysis. The values plotted are given in Table 6. A histogram of the residuals seemed normal as can be seen in Figure 11. The problem is that the value of both the ACF and PACF at lag three is now believed to be significant. Some minor improvements, such as a decrease in the standard deviation, have taken place by adding the second moving average term to the ARIMA(1,0,1) model, but these improvements are not significant.

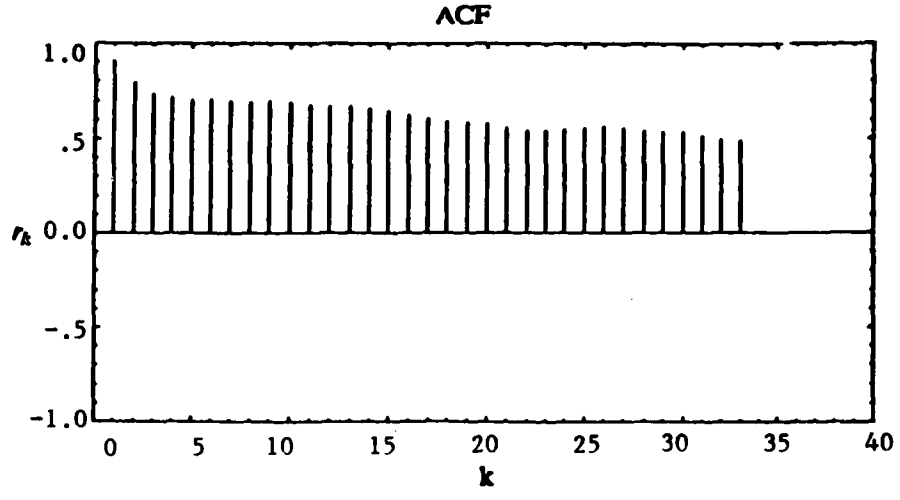

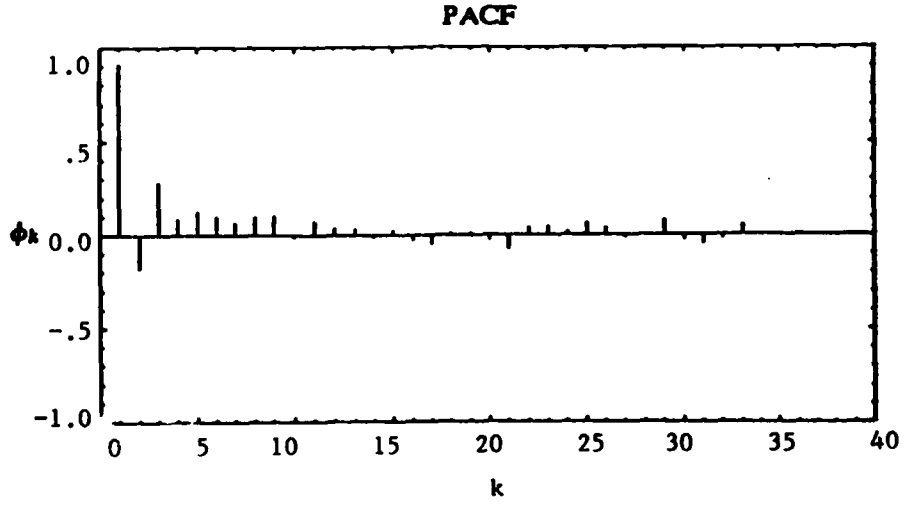

Figure 3. Estimated Autocorrelation (r_k) and Partial Autocorrelation Functions (ϕ_k) for the k th Lag of Radiometric Data.

TABLE 1

ESTIMATED AUTOCORRELATION AND PARTIAL AUTOCORRELATION FUNCTIONS OF RADIOMETRIC DATA

MEAN = 6.43
STANDARD DEVIATION = .0595

ACF

670 Observations

		1	2	3	4	5	6	7	8	9	10
r_k Lags	1-10	.909	.797	.739	.716	.707	.703	.697	.694	.698	.691
	11-20	.680	.673	.668	.656	.643	.628	.606	.590	.583	.577
	21-30	.558	.544	.545	.551	.558	.563	.557	.544	.542	.537
	31-33	.519	.499	.494							

PACF

670 Observations

		1	2	3	4	5	6	7	8	9	10
ϕ_k Lags	1-10	.909	-.177	.281	.086	.127	.100	.066	.097	.103	-.010
	11-20	.070	.040	.032	-.010	.017	-.027	-.046	.012	.007	-.017
	21-30	-.074	.038	.044	.019	.063	.038	-.007	.000	.080	-.024
	31-33	-.049	-.019	.055							

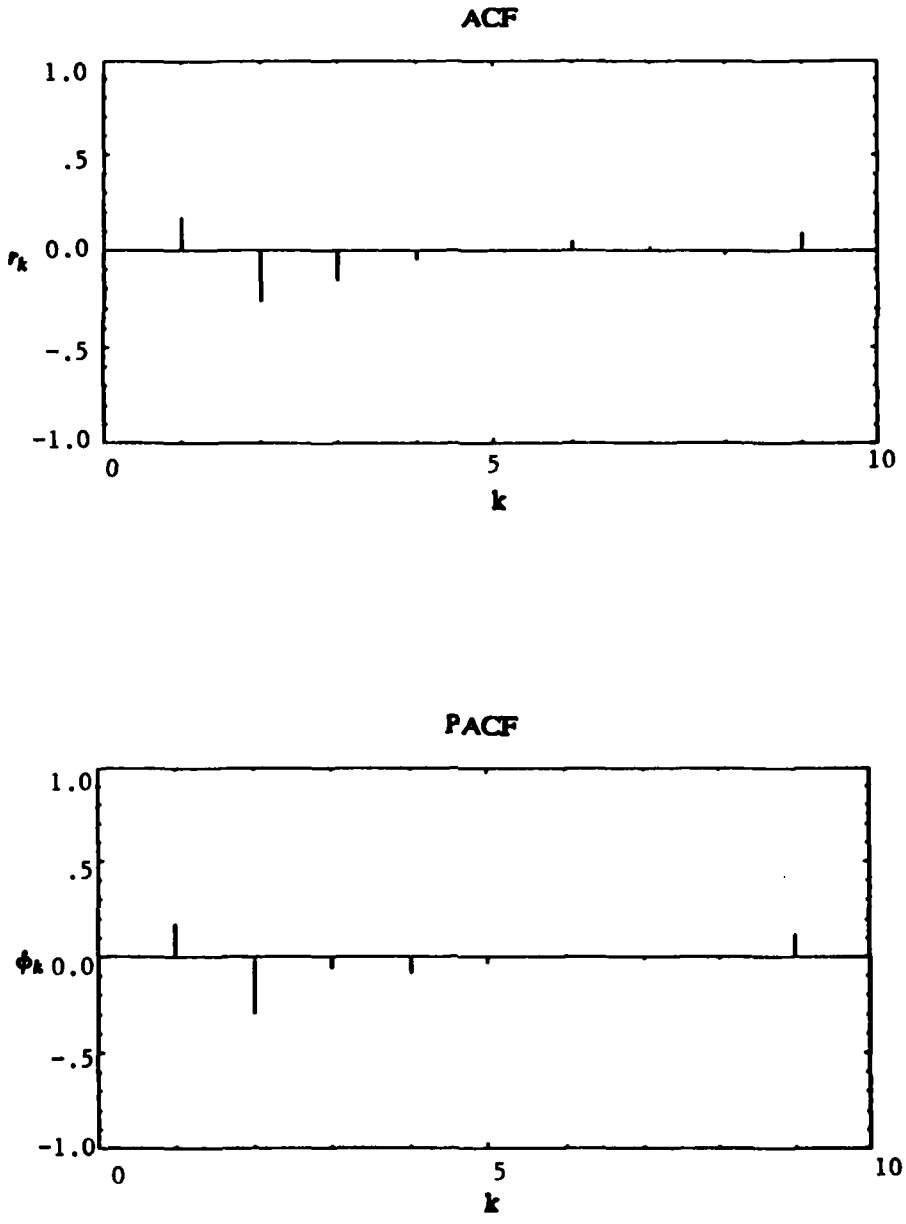

Figure 4. Plot of the Estimated ACF(r_k) and PACF(ϕ_k) of Residuals (ARIMA(1,0,0)) for the k th lag.

TABLE 2

ESTIMATED AUTOCORRELATION AND PARTIAL AUTOCORRELATION FUNCTIONS OF RESIDUALS
(ARIMA(1,0,0))

MEAN = -.0000301
STANDARD DEVIATION = .0245

ACF

670 Observations

		1	2	3	4	5	6	7	8	9
r_k Lags	1-9	.169	-.262	-.159	-.044	.006	.043	.019	-.019	.095

PACF

670 Observations

		1	2	3	4	5	6	7	8	9
ϕ_k Lags	1-9	.169	-.299	-.057	-.087	-.034	.006	-.015	-.016	.121

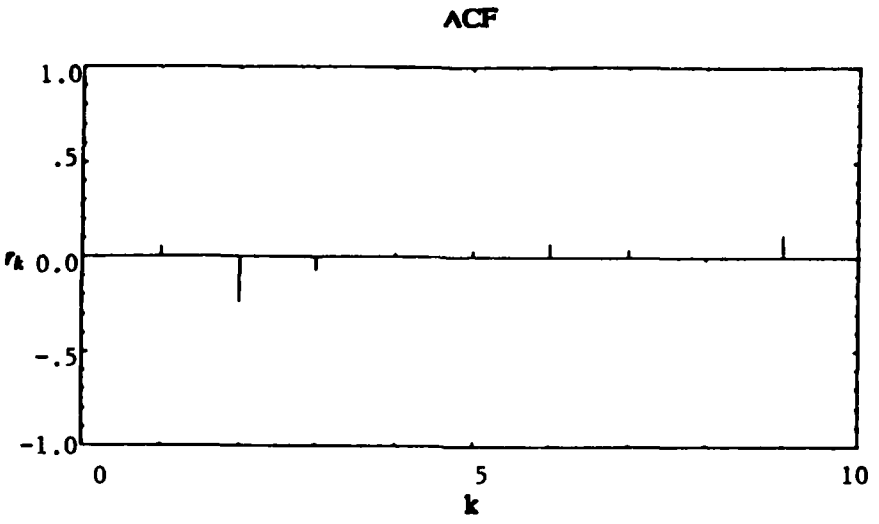

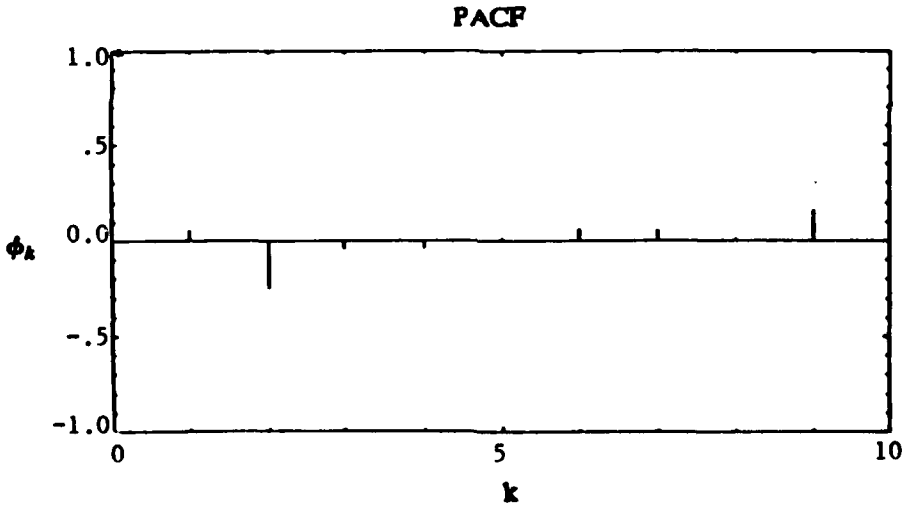

Figure 5. Plot of the Estimated ACF(r_k) and PACF(ϕ_k) of Residuals (ARIMA(2,0,0)) for the k th lag.

TABLE 3

ESTIMATED AUTOCORRELATION AND PARTIAL AUTOCORRELATION FUNCTIONS OF RESIDUALS (ARIMA(2,0,0))

MEAN = -.0000174
STANDARD DEVIATION = .0241

ACF

670 Observations

		1	2	3	4	5	6	7	8	9
r_k Lags	1-9	.053	-.242	-.070	.016	.035	.068	.042	-.019	.116

PACF

670 Observations

		1	2	3	4	5	6	7	8	9
ϕ_k Lags	1-9	.053	-.246	-.044	-.040	.009	.061	.047	.011	.157

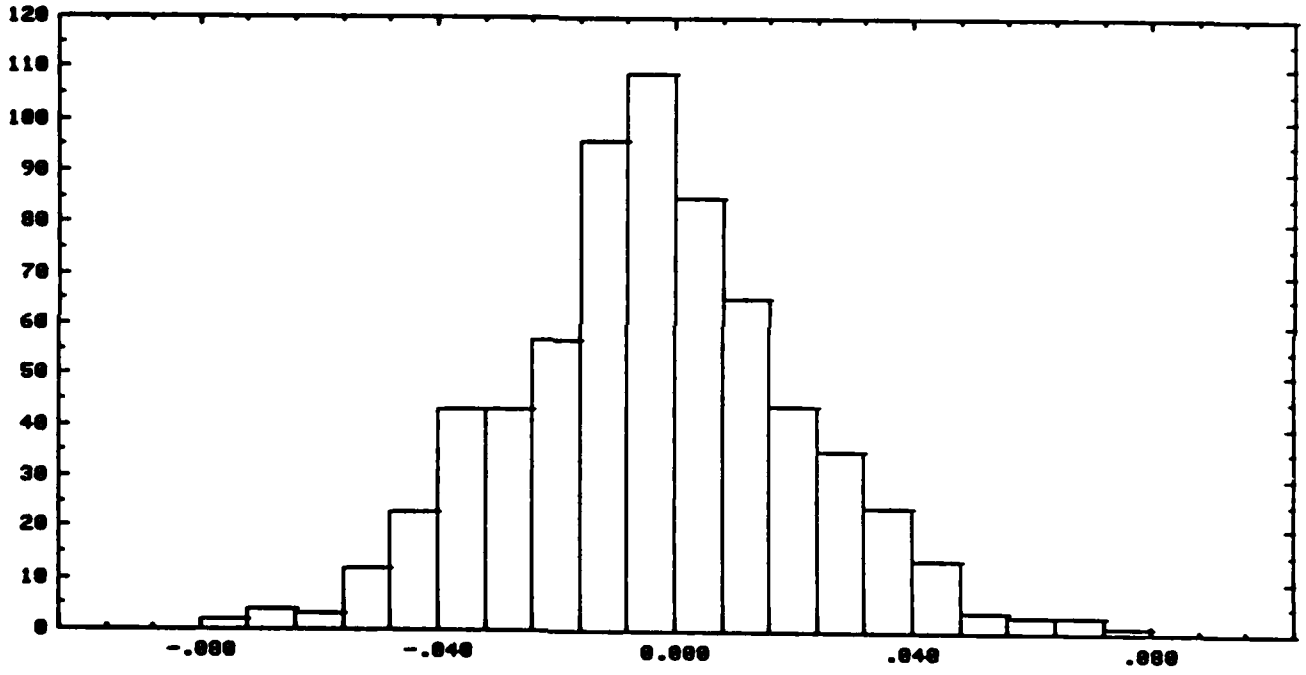

Figure 6. Histogram of Residuals of the ARIMA(2,0,0).

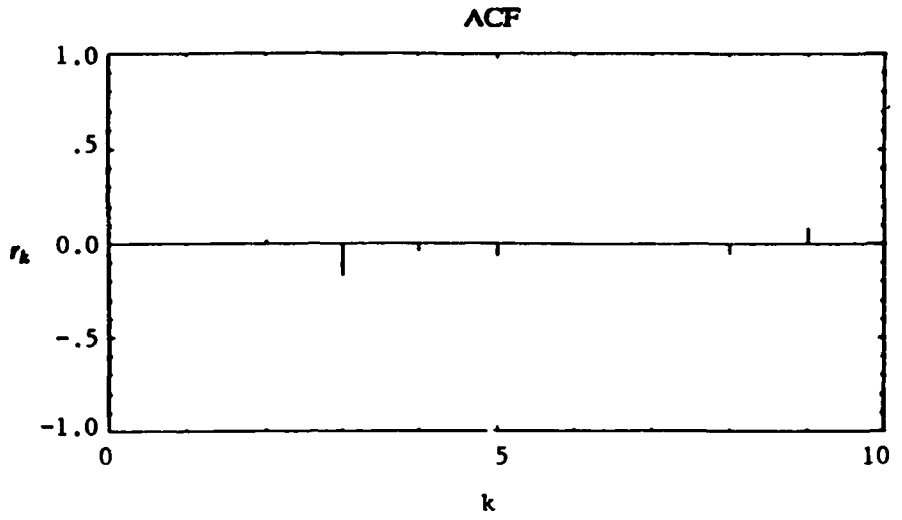

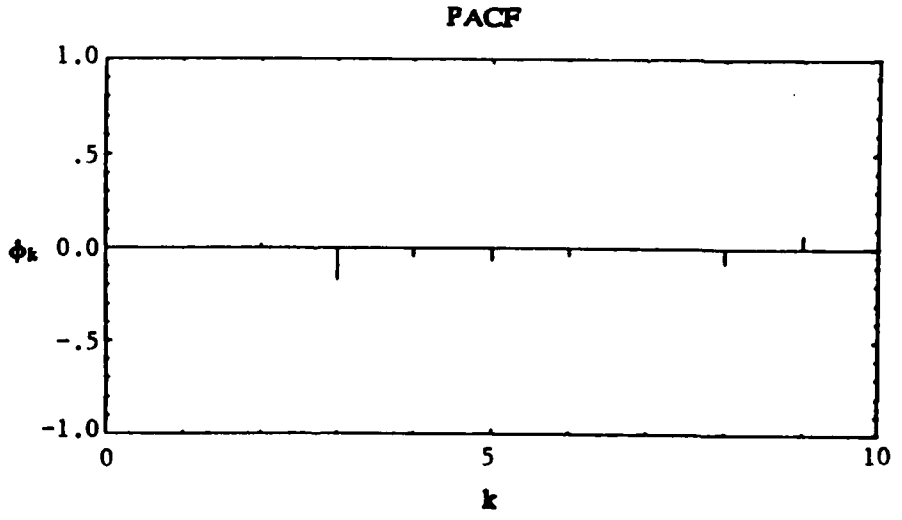

Figure 7. Plot of Estimated ACF(r_k) and PACF(ϕ_k) of Residuals (ARIMA(2,0,(2))) for the k th Lag.

TABLE 4

ESTIMATED AUTOCORRELATION AND PARTIAL AUTOCORRELATION FUNCTIONS OF RESIDUALS (ARIMA(2,0,(2)))

MEAN = -.0000403
STANDARD DEVIATION = .0229

ACF

670 Observations

		1	2	3	4	5	6	7	8	9
r_k Lags	1-9	-.005	.020	-.172	-.041	-.068	-.008	.004	-.052	.086

PACF

670 Observations

		1	2	3	4	5	6	7	8	9
ϕ_k Lags	1-9	-.005	.020	-.172	-.043	-.064	-.038	-.009	-.079	.074

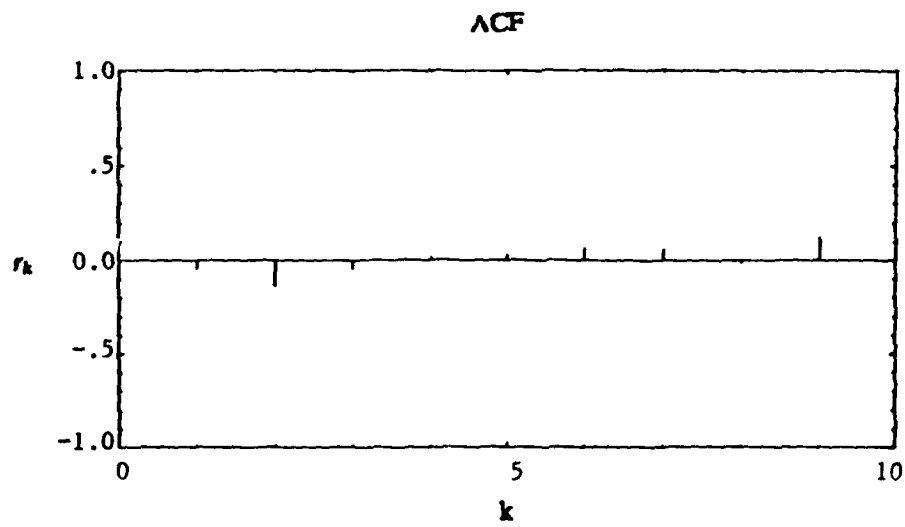

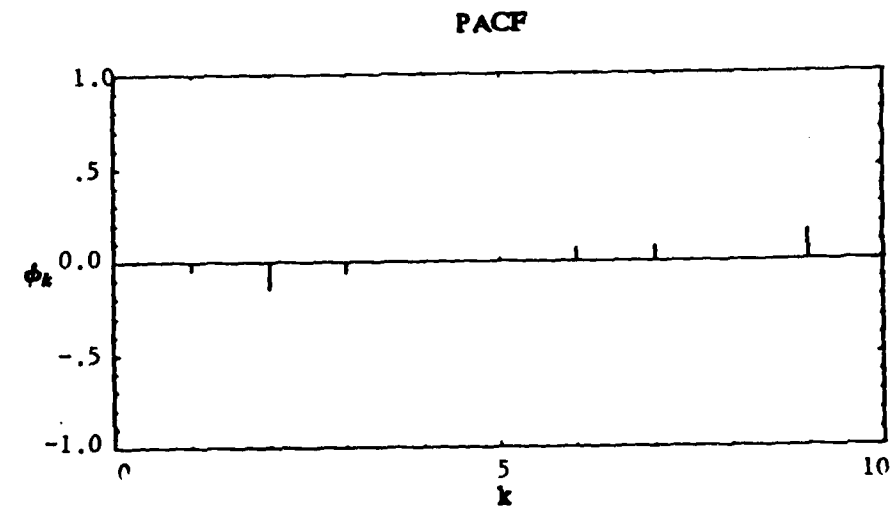

Figure 8. Plot of Estimated ACF(r_k) and PACF(ϕ_k) of Residuals (ARIMA(1,0,1)) for the k th Lag.

TABLE 5

ESTIMATED AUTOCORRELATION AND PARTIAL AUTOCORRELATION FUNCTIONS OF RESIDUALS
(ARIMA(1,0,1))

MEAN = -.0000150
STANDARD DEVIATION = .0237

ACF

670 Observations

		1	2	3	4	5	6	7	8	9
r_k Lags	1-9	-.047	-.141	-.045	.021	.036	.066	.059	-.023	.128

PACF

670 Observations

		1	2	3	4	5	6	7	8	9
ϕ_k Lags	1-9	-.047	-.144	-.061	-.005	.022	.071	.079	.009	.158

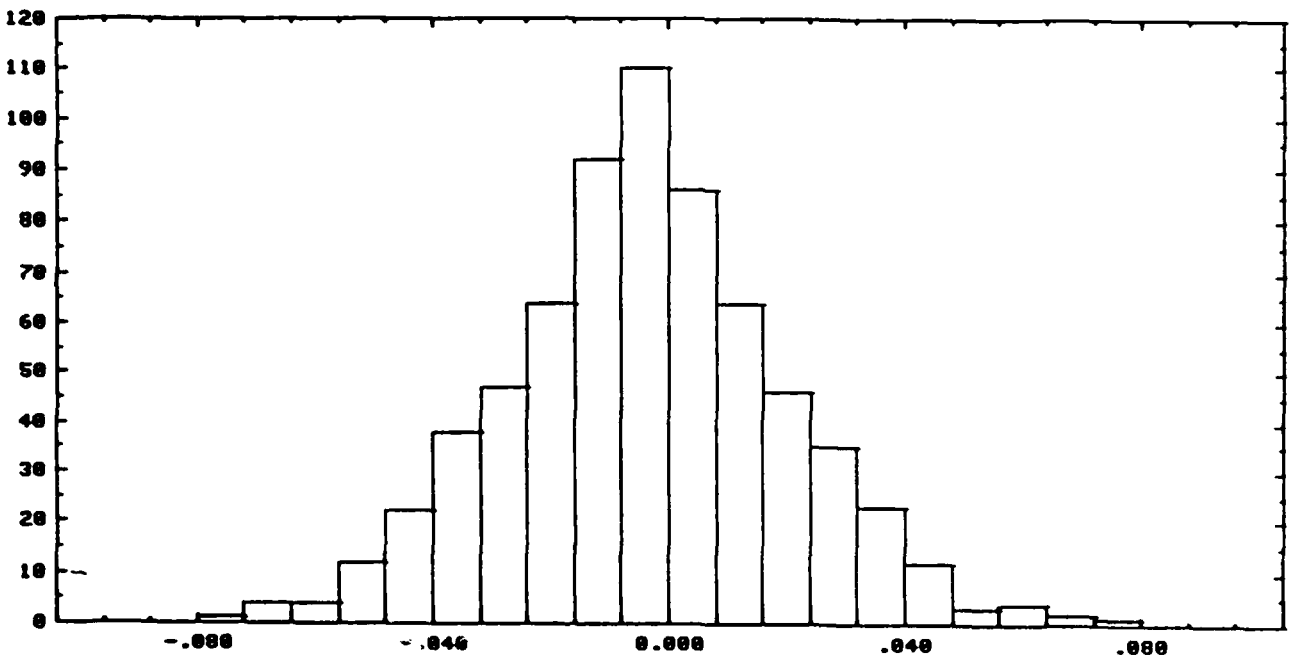

Figure 9. Histogram of Residuals of the ARIMA(1,0,1).

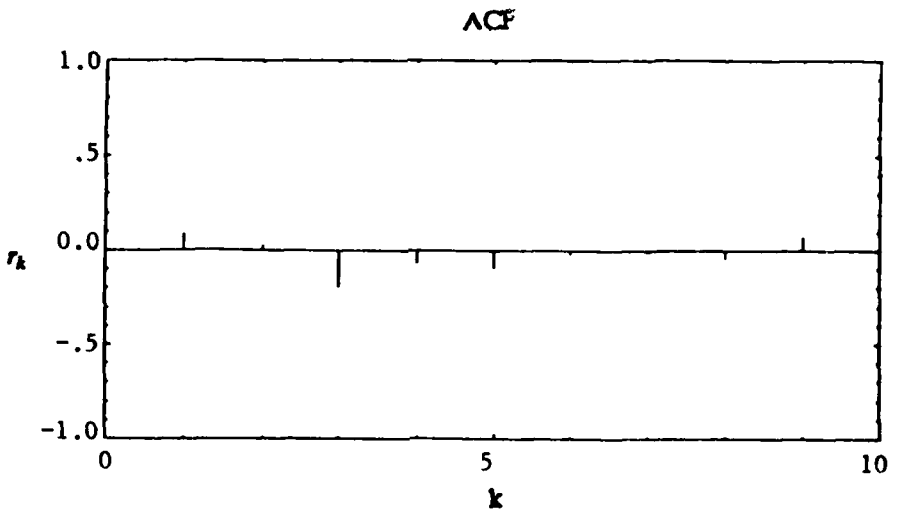

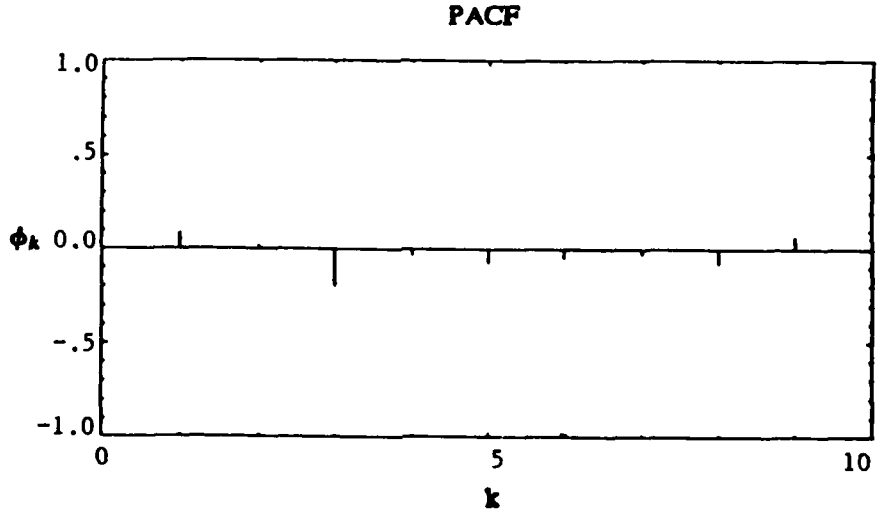

Figure 10. Plot of Estimated ACF(r_k) and PACF(ϕ_k) of Residuals (ARIMA(1,0,2)) for the k th Lag.

TABLE 6

ESTIMATED AUTOCORRELATION AND PARTIAL AUTOCORRELATION FUNCTIONS OF RESIDUALS
(ARIMA(1,0,2))

MEAN = -.0000429
STANDARD DEVIATION = .0231

ACF

670 Observations

		1	2	3	4	5	6	7	8	9
r_k Lags	1-9	.087	.025	-.194	-.068	-.092	-.022	-.013	-.047	.075

PACF

670 Observations

		1	2	3	4	5	6	7	8	9
ϕ_k Lags	1-9	.087	.018	-.199	-.036	-.075	-.046	-.024	-.082	.068

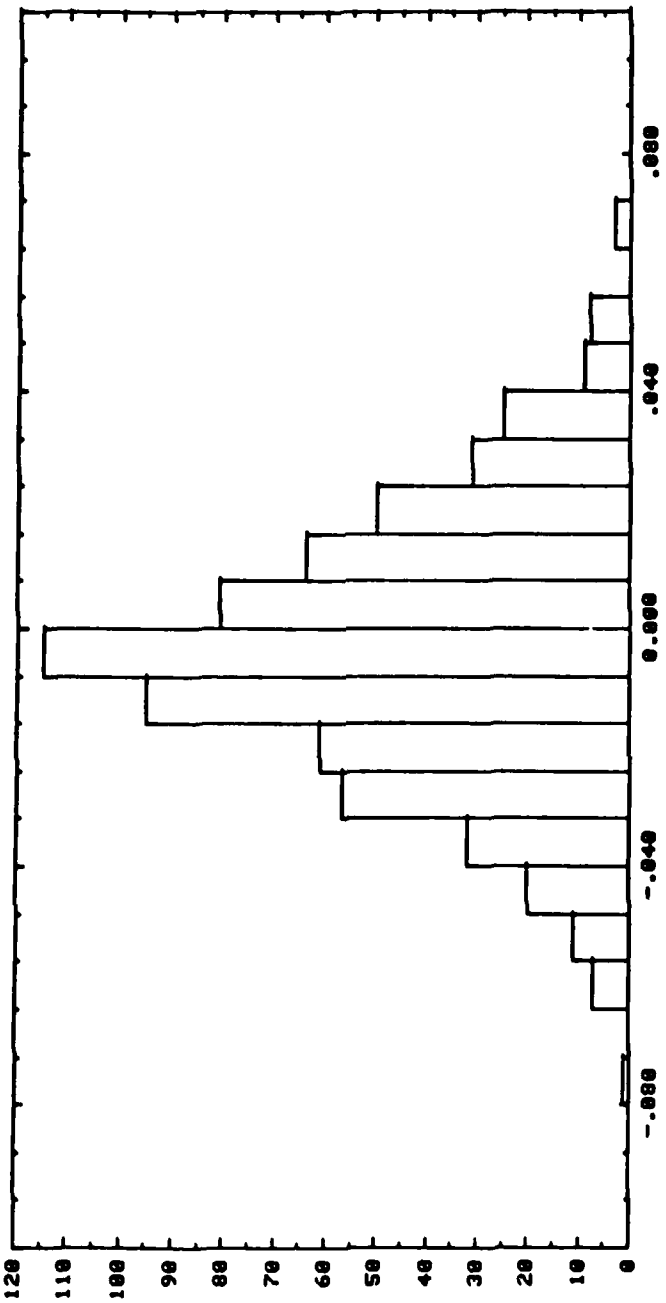

Figure 11. Histogram of Residuals of ARIMA(1,0,2).

Nevertheless, the ARIMA(1,0,3) model was tentatively used to remove the significant values of both the ACF and PACF at the third lag. A plot of the ACF and PACF of the residuals is shown in Figure 12, with the values given in Table 7. After all these modeling attempts, the ARIMA(1,0,3) model seems to characterize the radiometric data best. Both the ACF and PACF of the residuals seem small and the standard deviation of 0.0224. is smaller than any other model that was studied as can be seen in Table 8.

At this point in the analysis a reflection on the ability of each tentative model to characterize this data parsimoniously should be addressed. Although the ARIMA(1,0,3) may be slightly better than the other models, a summary of the ARIMA models in terms of parameters and residuals indicates that the ARIMA(1,0,1) structure is almost as good as any other satisfactory model, and it only requires two parameters. **Therefore, based on the principle of parsimony the ARIMA(1,0,1) model was chosen to characterize the radiometric data.**

If the following definitions are made

$$a_t \approx N(0,\sigma_a{}^2)\,, \tag{III.1}$$

and

$$\tilde{Z}_t = Z_t - \mu\,, \tag{III.2}$$

where the mean of Z_t is μ, then the ARIMA(1,0,1) becomes

$$(1-\phi_1 B)\tilde{Z}_t = (1-\theta_1 B)a_t\,, \tag{III.3}$$

where the backward shift operator B is defined as $B\tilde{Z}_t = \tilde{Z}_{t-1}$, and $Ba_t = a_{t-1}$. If Equation (III.3) is expanded and rearranged, then in terms of the original data Z_t becomes

$$Z_t = (1-\phi_1)\mu + \phi_1 Z_{t-1} + a_t - \theta_1 a_{t-1}\,. \tag{III.4}$$

IV MILLIMETER-WAVE (MMW) RADAR ANALYSIS

The radar data was collected simultaneously with the radiometer data at APG, Md. The radar is an active sensor, which means that it sends out a signal that is scattered off objects on the ground and back into its receiving antenna. On the other hand the radiometer does not send signals, but only receives them from the ground; hence it is referred to as a passive sensor. Uncalibrated signals from the radar sensor are presented in Figure 13. To obtain the calibrated radar data of Figure 2 the zero cross section reference level (2.95) of the uncalibrated data must be substracted from each uncalibrated data point and the result multiplied by a calibration constant of 8.0 square meters per unit.

Figure 14 is a histogram of the uncalibrated radar data, which shows the skewness of these signals. It is obvious that the deviations are not symmetric about the mean as well as having positive deviations larger in magnitude than those in the negative direction. Because of this skewness in the radar data, a data transformation was necessary to best

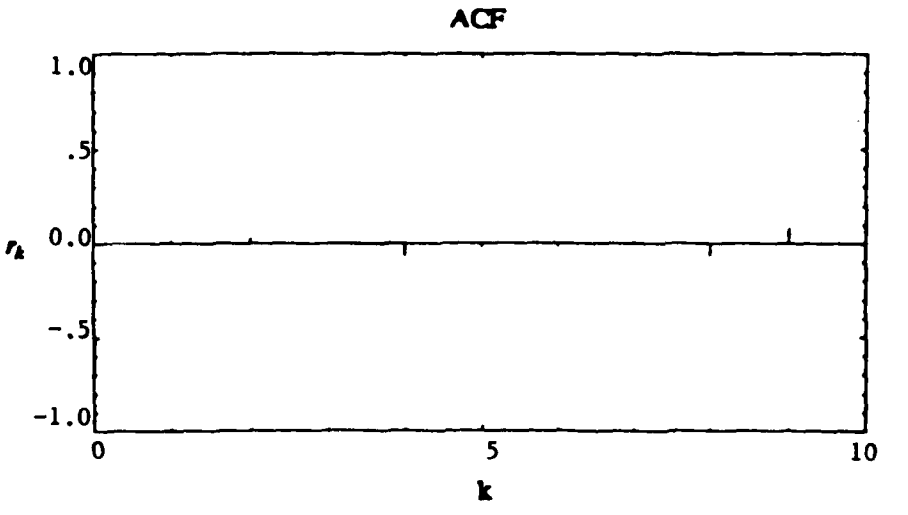

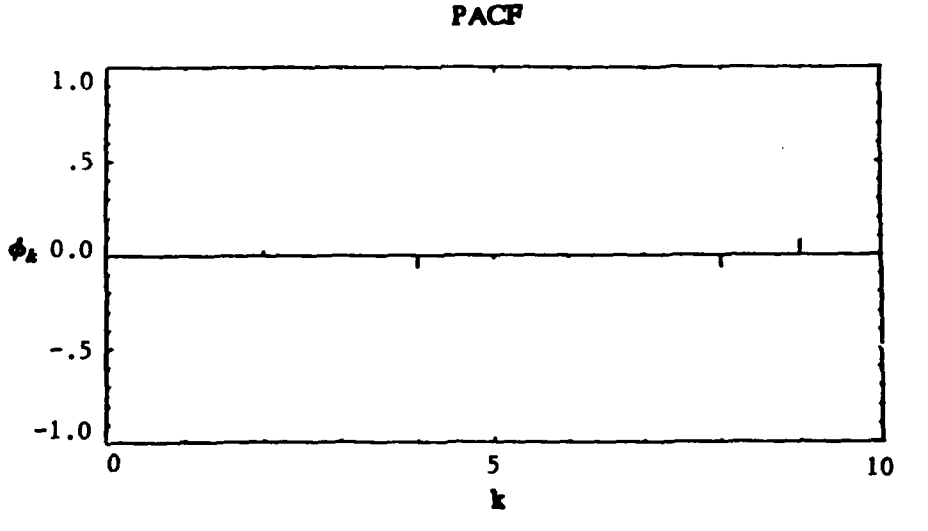

Figure 12. Plot of Estimated ACF(r_k) and PACF(ϕ_k) of Residuals (ARIMA(1,0,3)) for the k th Lag.

TABLE 7

ESTIMATED AUTOCORRELATION AND PARTIAL AUTOCORRELATION FUNCTIONS OF RESIDUALS
(ARIMA(1,0,3))

MEAN = -.0000469
STANDARD DEVIATION = .0224

ACF

670 Observations

		1	2	3	4	5	6	7	8	9
r_k Lags	1-9	.012	.025	-.001	-.067	-.018	-.017	.010	-.063	.079

PACF

670 Observations

		1	2	3	4	5	6	7	8	9
ϕ_k Lags	1-9	.012	.025	-.001	-.068	-.017	-.013	.011	-.068	.078

TABLE 8

SUMMARY OF ARIMA(•) MODELS ENTERTAINED FOR PASSIVE SENSORS
(BACKCASTING METHOD)

	ARIMA(p,d,q) (p,d,q)	ESTIMATED PARAMETERS	WHITE NOISE	NOTE
(1)	(1,0,1)	$\bar{\phi}_1 = 0.9127$	$\bar{a} = -.00003$	Some remaining structure in the
	centered		$S_a^+ = 0.0245$	residuals [AR(2) or MA(1)].
(2)	(2,0,0)	$\bar{\phi}_1 = 1.086$	$\bar{a} = -.000017$	ACF at Lag 2.
	centered	$\bar{\phi}_2 = -.1902$	$S_a = 0.0241$	
(3)	(2,0,(2))	$\bar{\phi}_1 = 1.0913$	$\bar{a} = -.00004$	ACF at Lag 3.
	centered	$\bar{\phi}_2 = -.1274$	$S_a = 0.0229$	
		$\bar{\theta}_2 = 0.3866$		
(4)*	(1,0,1)	$\bar{\phi}_1 = 0.8537$	$\bar{a} = -.000015$	ACF at Lag 2 with PACF
	centered	$\bar{\theta}_1 = -.3569$	$S_a = 0.0237$	at Lag 2 with decay.
(5)	(1,0,2)	$\bar{\phi}_1 = 0.9676$	$\bar{a} = -.000043$	ACF at Lag 3.
	centered	$\bar{\theta}_1 = -.028$	$S_a = 0.0231$	
		$\bar{\theta}_2 = 0.4067$		
(6)	(1,0,3)	$\bar{\phi}_1 = 0.9874$	$\bar{a} = -.000947$	
	centered	$\bar{\theta}_1 = -.0654$	$S_a = 0.0224$	
		$\bar{\theta}_2 = 0.4342$		
		$\bar{\theta}_3 = 0.2492$		

+The symbol S_a is the estimated standard deviation.

*The ARIMA(1,0,1) results are as good as any above, and based on the principle of parsimony one would choose the p=1, d=0, q=1 model.

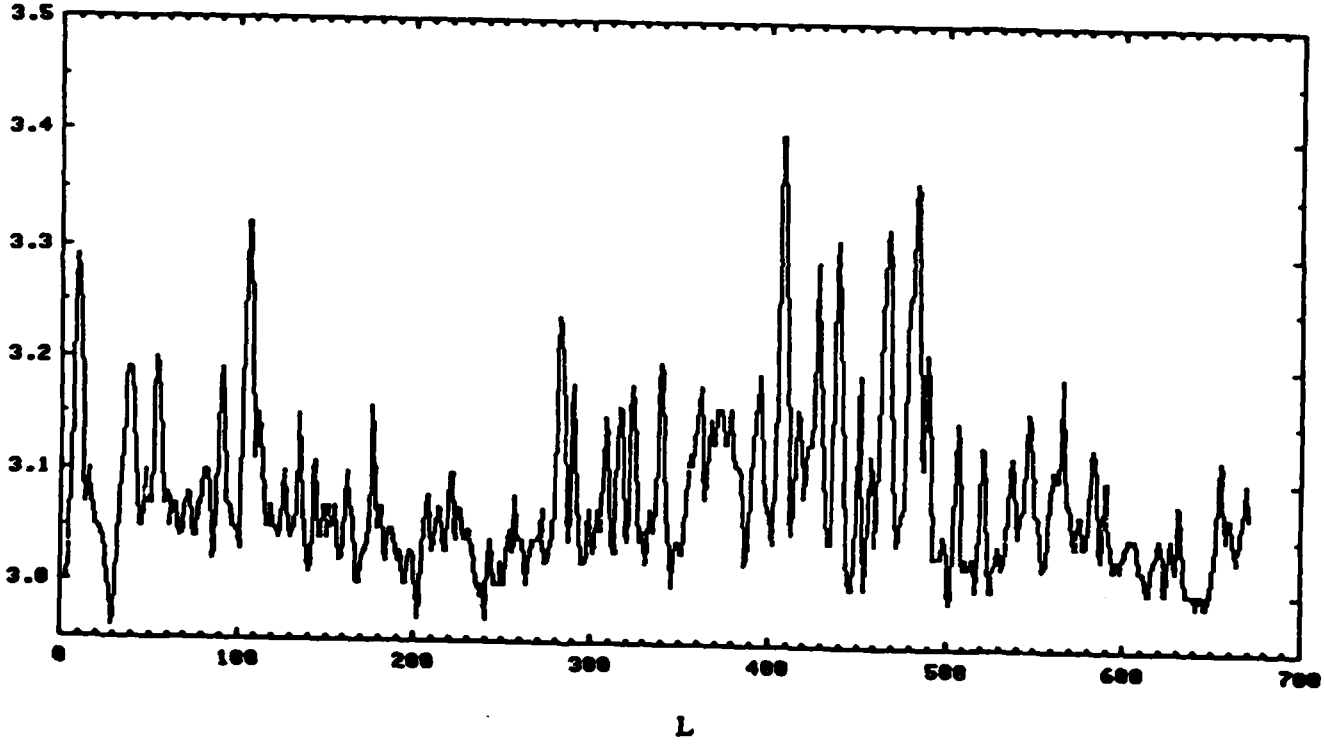

Figure 13. The Actual Uncalibrated Radar Data for a Field at 90m Slant Range is Plotted Against the Integer Number L of Time Steps, ($\Delta t = .5ms$).

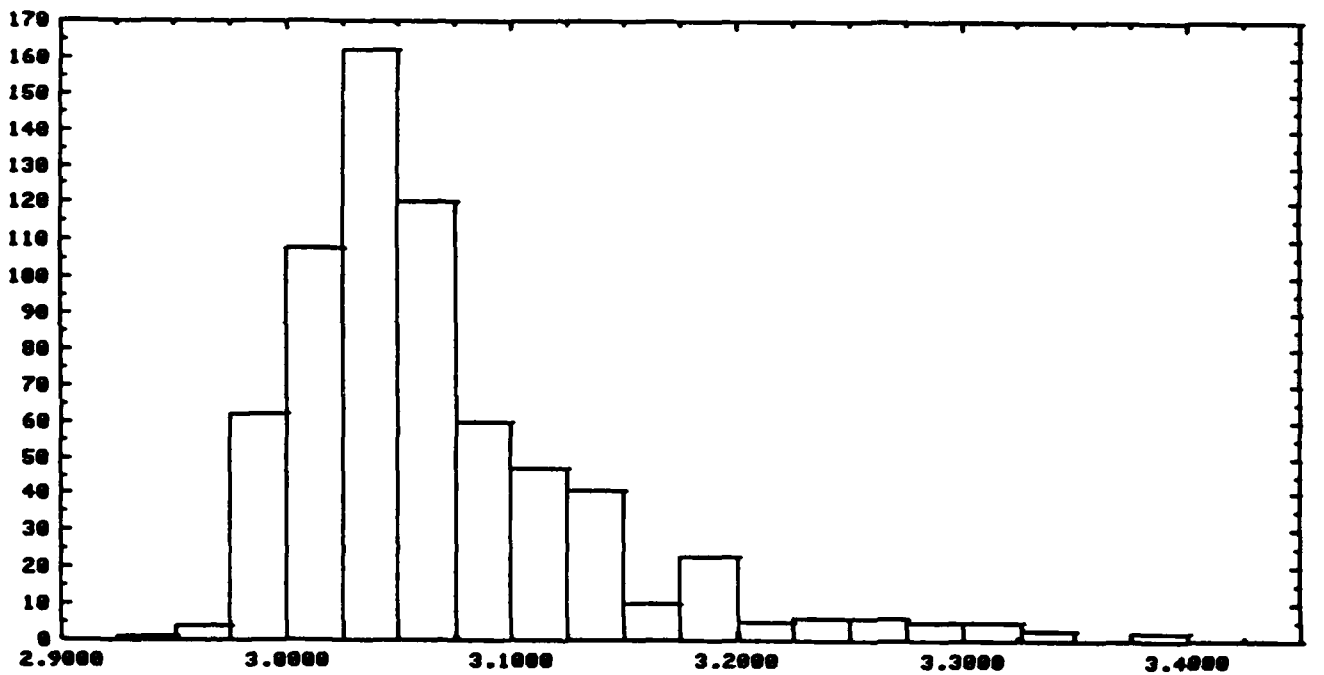

Figure 14. Histogram of the Actual Uncalibrated Radar Data.

utilize the Box and Jenkins method on this data set.

A natural logarithm (ln) transformation was selected to transform the radar data (Z_t) into a new variable (Y_t) in such a way that the new deviations are symmetric about their mean. This logarithm transformation maintains the order of the original data and symmetrically transforms the data to enhance the time series analysis.

The data transformation used is based upon a simple idea of equating the maximum and minimum distance from the mean value. Hence, take the maximum logarithm value of the observations minus the mean value and equate it to the mean logarithm value minus the minimum value. This procedure equates the magnitude of the maximum and minimum deviations from the mean, thereby improving the symmetric properties.

$$\max ln(\bullet) - mean\ ln(\bullet) = mean\ ln(\bullet) - \min ln(\bullet) . \qquad \text{(IV.1)}$$

or

$$ln(\ 3.40 + \Delta\ ) - ln(\ 3.08 + \Delta\ ) = ln(\ 3.08 + \Delta\ ) - ln(\ 2.96 + \Delta\ ) . \qquad \text{(IV.2)}$$

The solution for Δ is -2.89.

The transformation, $Y_t = ln(\ Z_t - 2.89\ )$, which is based on improving the symmetric properties, needs a second minor adjustment. This minor adjustment was a correction in the value of the parameter Δ to -2.91.

$$Y_t = ln(\ Z_t - 2.91\ ) , \qquad \text{(IV.3)}$$

where

$$mean\ Y_t = -1.85 ,$$

$$maximum\ Y_t = -.7134 ,$$

$$minimum\ Y_t = -2.995 ,$$

and

$$standard\ deviation\ S_Y = 0.370 .$$

More details of the evaluation of the parameter Δ are given in Appendix A.

A nice property of this ln(•) transformation is that the order of the observations remain the same as the original data. Hence, the ACF and PACF of the original observation as well as the transformed data are similar. This similarity can be seen by comparing Figure 15 with Figure 16. The values plotted are listed in Table 9 and Table 10, respectively.

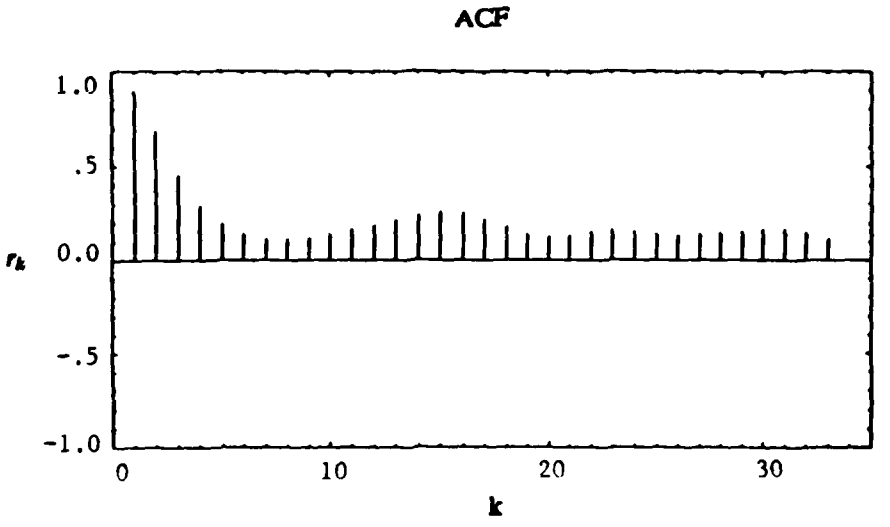

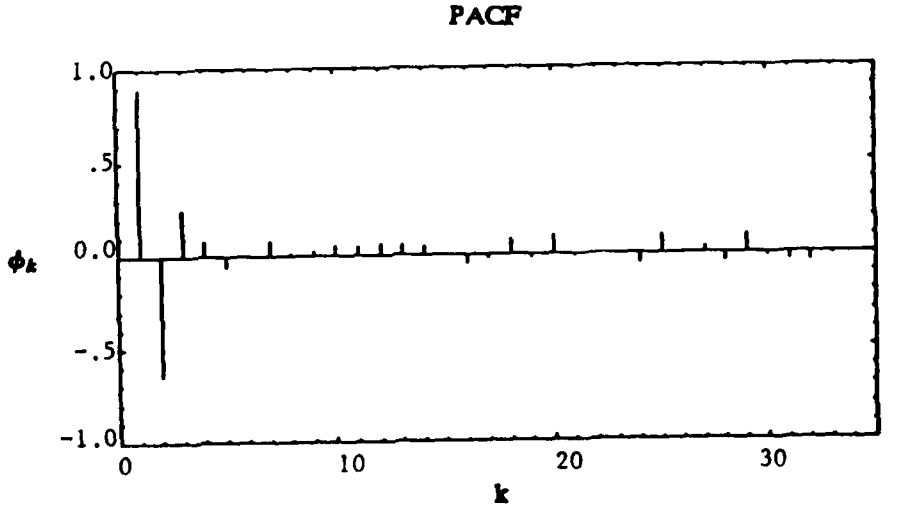

Figure 15. Estimated Autocorrelation (r_k) and Partial Autocorrelation Functions (ϕ_k) for the k th Lag of Radar Data.

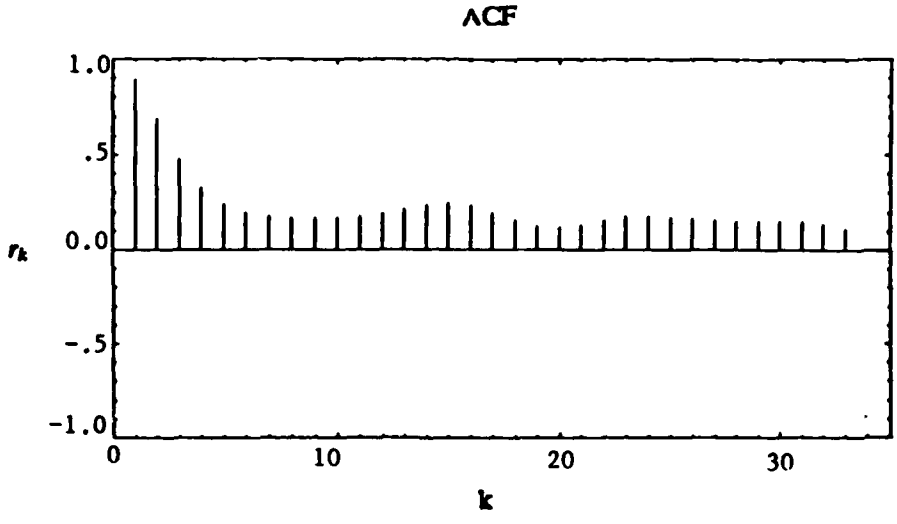

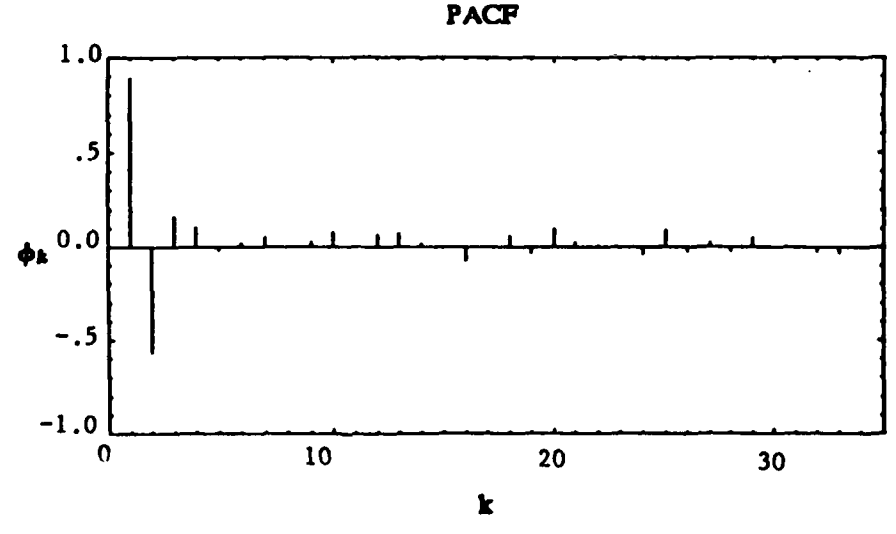

Figure 16. Estimated Autocorrelation (r_k) and Partial Autocorrelation Functions (ϕ_k) for the k th Lag of Transformed Radar Data.

TABLE 9

ESTIMATED AUTOCORRELATION AND PARTIAL AUTOCORRELATION FUNCTIONS OF RADAR DATA

MEAN = 3.08
STANDARD DEVIATION = .0697

ACF

670 Observations

		1	2	3	4	5	6	7	8	9	10
r_k Lags	1-10	.898	.682	.457	.289	.189	.135	.113	.111	.121	.140
	11-20	.162	.187	.213	.239	.256	.252	.220	.178	.141	.127
	21-30	.134	.150	.159	.152	.138	.130	.135	.143	.153	.162
	31-33	.164	.147	.112							

PACF

670 Observations

		1	2	3	4	5	6	7	8	9	10
ϕ_k Lags	1-10	.898	-.647	.253	.081	-.062	.009	.082	.016	.028	.054
	11-20	.045	.057	.054	.048	.001	-.046	-.019	.081	-.019	.097
	21-30	-.011	.002	-.003	-.055	.101	-.004	.034	-.046	.096	-.019
	31-33	-.040	-.044	-.013							

TABLE 10

ESTIMATED AUTOCORRELATION AND PARTIAL AUTOCORRELATION FUNCTIONS OF TRANSFORMED RADAR DATA

MEAN = -1.85
STANDARD DEVIATION = .370

ACF

670 Observations

		1	2	3	4	5	6	7	8	9	10
r_k Lags	1-10	.895	.689	.481	.330	.242	.196	.178	.171	.168	.171
	11-20	.180	.194	.215	.237	.250	.237	.198	.157	.125	.117
	21-30	.132	.158	.179	.179	.171	.162	.158	.154	.153	.154
	31-33	.151	.137	.111							

PACF

670 Observations

		1	2	3	4	5	6	7	8	9	10
ϕ_k Lags	1-10	.895	-.567	.164	.103	-.018	.022	.054	-.002	.029	.079
	11-20	.002	.065	.071	.022	-.006	-.070	.006	.060	-.030	.096
	21-30	.025	.014	-.007	-.041	094	-.026	.025	-.024	.054	-.002
	31-33	-.009	- .028	-.035							

The sinusoidal pattern in the ACF and the cutoff pattern in the PACF indicate some type of autoregressive (AR) process. A second order autoregressive model was therefore entertained. The values of the ACF and PACF for the residuals are plotted in Figure 17, and displayed in Table 11.

Although Table 11 indicates a reasonable degree of success, the residuals plotted as a histogram in Figure 18 indicated that the residuals were not gaussian (normal). Hence, the residuals did not satisfy the basic assumption in the Box and Jenkins method that is explained in more detail in their book[1].

To improve upon the time series model a number of moving average terms were introduced into the analysis to remove any significant value of the ACF and PACF that may exist at the different lags, as well as to satisfy the underlying white noise assumptions of normality ($N(0,\sigma_a^2)$). See Table 12 for a breakdown of the ARIMA time series analysis attempted during this investigation.

The ARIMA(2,0,(2,3,4)) process was able to characterize the millimeter wave radar data well, where the random shock was truly random and symmetric as Figure 19 indicates. The question that always arises in this type of modeling effort is how general is this particular ARIMA model. In order to answer such a question , some sets of observations other than those already reported on were analyzed with the same ARIMA model. The results are reported in Table 13.

This particular time series structure was able to characterize the other data sets, where the estimated parameters remained relatively the same, indicating some degree of generality of this time series process.

If the following definitions are made,

$$a_t \approx N(0,\sigma_a^2)\,, \tag{IV.4}$$

and

$$W_t = Y_t - \mu\,, \tag{IV.5}$$

where the mean of Y_t is μ , then the ARIMA(2,0,(2,3,4)) becomes

$$(1 - \phi_1 B - \phi_2 B^2)W_t = (1 - \theta_2 B^2 - \theta_3 B^3 - \theta_4 B^4)a_t\,, \tag{IV.6}$$

where the backward shift operator B is defined as $BW_t = W_{t-1}$,and $Ba_t = a_{t-1}$. If Equation (IV.6) is expanded and rearranged,

$$W_t = \phi_1 W_{t-1} + \phi_2 W_{t-2} + a_t - \theta_2 a_{t-2} - \theta_3 a_{t-3} - \theta_4 a_{t-4}\,, \tag{IV.7}$$

thus, Y_t becomes

$$Y_t = \mu + \phi_1(Y_{t-1} - \mu) + \phi_2(Y_{t-2} - \mu) + a_t - \theta_2 a_{t-2} - \theta_3 a_{t-3} - \theta_4 a_{t-4}\,. \tag{IV.8}$$

Finally, in terms of the original data Z_t becomes

$$Z_t = e^{Y_t} + 2.91\,. \tag{IV.9}$$

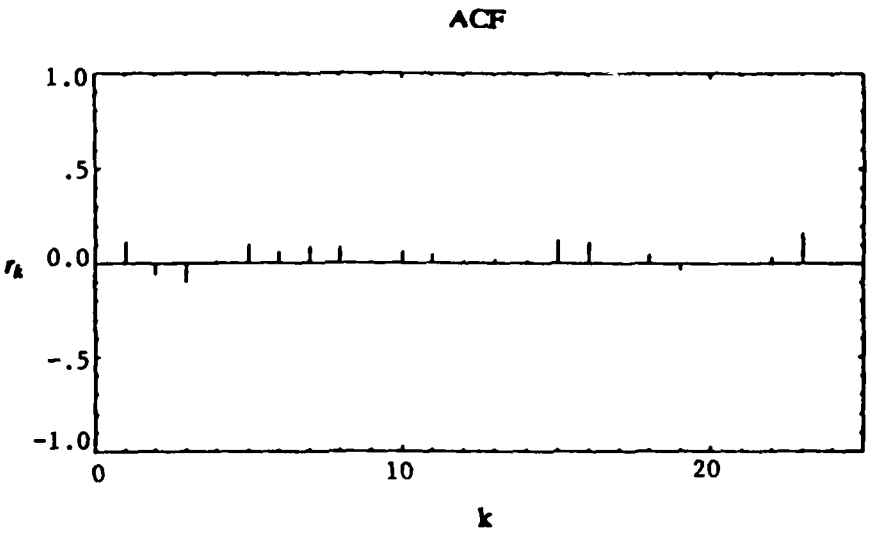

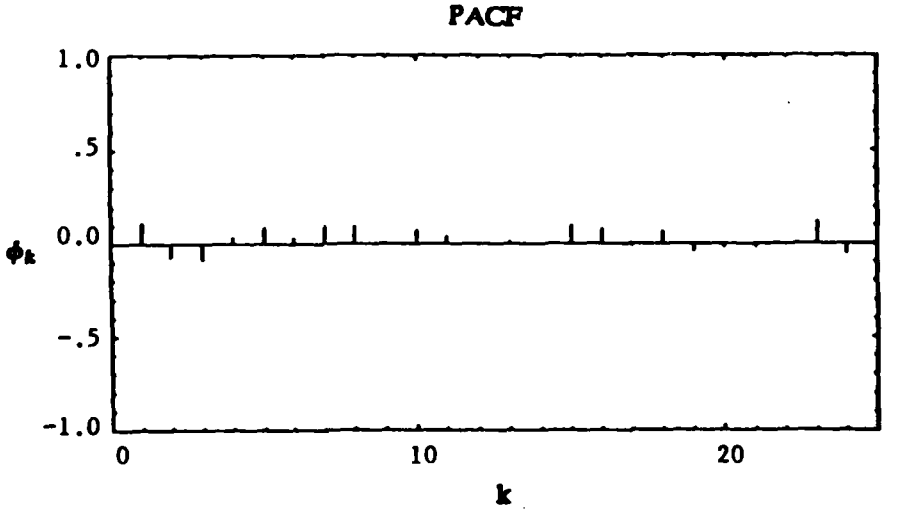

Figure 17. Plot of Estimated ACF(r_k) and PACF(ϕ_k) of Residuals (ARIMA(2,0,0)) for the k th Lag of Transformed Radar Data.

TABLE 11

ESTIMATED AUTOCORRELATION AND PARTIAL AUTOCORRELATION FUNCTIONS OF RESIDUALS OF TRANSFORMED RADAR DATA (ARIMA(2,0,0))

MEAN = .0000668
STANDARD DEVIATION = 0.133

ACF

670 Observations

		1	2	3	4	5	6	7	8	9	10
r_k Lags	1-10	.110	-.060	-.101	.012	.101	.060	.087	.084	.008	.057
	11-20	.044	.015	.022	.016	.119	.112	.008	.048	-.031	.001
	21-24	.007	.031	.161	-.008						

PACF

670 Observations

		1	2	3	4	5	6	7	8	9	10
ϕ_k Lags	1-10	.110	-.073	-.088	.030	.087	.033	.094	.091	.006	.075
	11-20	.040	-.006	.016	.003	.096	.081	-.011	.065	-.038	-.018
	21-24	-.019	-.006	.121	-.054						

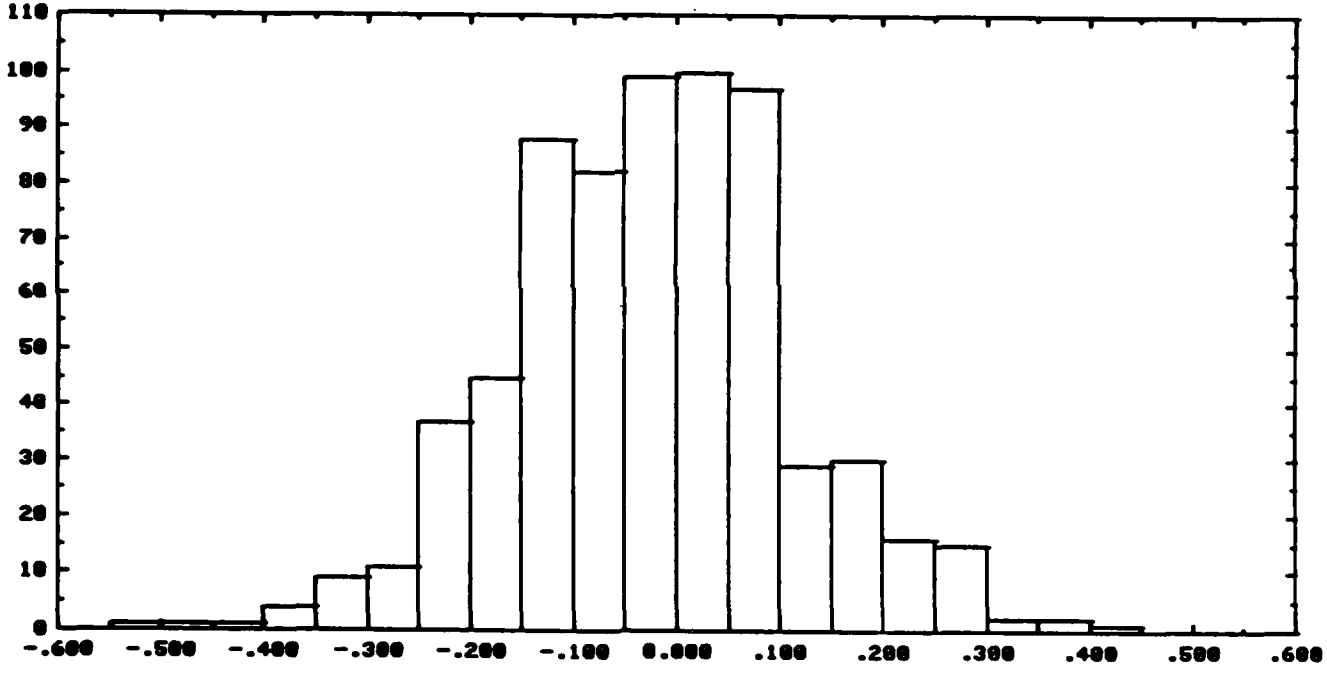

Figure 18. Histogram of Residuals of ARIMA(2,0,0) for the Transformed Radar Data.

TABLE 12

SUMMARY OF ARIMA MODELS FOR TRANSFORMED RADAR DATA BY BACKCASTING METHOD+
($Y_t = ln(Z_t - 2.91); \bar{Y} = -1.85, S_Y = 0.37$)

	ARIMA(p,d,q) (p,d,q)	ESTIMATED PARAMETERS	WHITE NOISE	NOTE
(1)	(2,0,0)	$\bar{\phi}_1 = 1.4309$	$\bar{a} = .000067$	Significant value for ACF and PACF at Lag(1).
	Centered	$\bar{\phi}_2 = -.5962$	$S_a = 0.133$	
(2)	(2,0,1)	$\bar{\phi}_1 = 1.2816$	$\bar{a} = -.000061$	Residuals* not normal, $N(0,\sigma_a^2)$.
	Centered	$\bar{\phi}_2 = -.4638$	$S_a = 0.131$	
		$\bar{\theta}_1 = -.2435$		
(3)	(2,0,2)	$\bar{\phi}_1 = 1.0331$	$\bar{a} = -.000061$	Residuals* not normal, $N(0,\sigma_a^2)$
	Centered	$\bar{\phi}_2 = -.2715$	$S_a = 0.130$	
		$\bar{\theta}_1 = -.4995$		
		$\bar{\theta}_2 = -.2381$		
(4)	(2,0,(2,3))	$\bar{\phi}_1 = 1.5021$	$\bar{a} = -.000061$	Residuals* not normal, $N(0,\sigma_a^2)$
	Centered	$\bar{\phi}_2 = -.5787$	$S_a = .131$	Significant value of ACF and PACF at Lag(4).
		$\bar{\theta}_2 = .1790$		
		$\bar{\theta}_3 = .2445$		
(5)	(2,0,(2,3,4))	$\bar{\phi}_1 = 1.5261$	$\bar{a} = -.00112$	Residuals are normal, $N(0,\sigma_a^2)$.
	Centered	$\bar{\phi}_2 = -.5339$	$S_a = 0.129$	The ACF and PACF are well behaved.
		$\bar{\theta}_2 = .2920$		
		$\bar{\theta}_3 = .3870$		
		$\bar{\theta}_4 = .2007$		

+BMDQ2T (TSPACK) Time Series Package; Program Revised July 1, 1979 ,Copyright (c) 1979,Regents of University of California. (Storage 16000.)

*The histogram of the residuals indicates that the normality assumption for the Box and Jenkins ARIMA process does not hold.

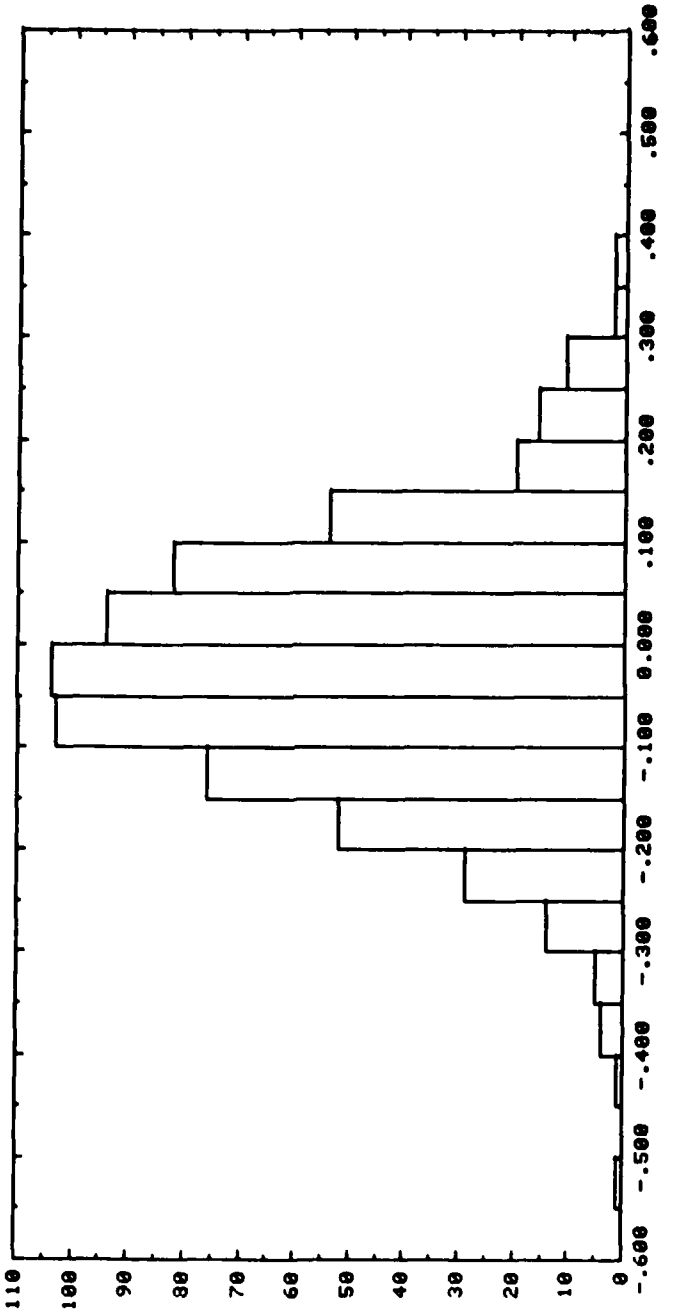

Figure 19. Histogram of Residuals of ARIMA(2,0,(2,3,4)) for the Transformed Radar Data.

TABLE 13

OTHER DATA SETS
(BACKCASTING METHOD)

	ARIMA(p,d,q) (p,d,q)	ESTIMATED PARAMETERS	WHITE NOISE	NOTE
(1)	(2,0,(2,3,4))	$\bar{\phi}_1 = 1.5261$	$\bar{a} = -.00112$	Histogram of Residuals ~ $N(0,\sigma_a^2)$*
	Centered	$\bar{\phi}_2 = -.5339$	$S_a = 0.129$	The ACF and PACF are well behaved .
	$\bar{Y} = -1.85$	$\bar{\theta}_2 = 0.2920$		
	$S_Y = 0.370$	$\bar{\theta}_3 = 0.3870$		
		$\bar{\theta}_4 = 0.2007$		
(2)	(2,0,(2,3,4))	$\bar{\phi}_1 = 1.5273$	$\bar{a} = -.00121$	~$N(0,\sigma_a^2)$
	Centered	$\bar{\phi}_2 = -.5360$	$S_a = 0.126$	The ACF and PACF are well behaved.
	$\bar{Y} = -1.88$	$\bar{\theta}_2 = 0.3807$		
	$S_Y = 0.338$	$\bar{\theta}_3 = 0.3505$		
		$\bar{\theta}_4 = 0.1469$		
(3)	(2,0,(2,3,4))	$\bar{\phi}_1 = 1.5026$	$\bar{a} = -.00049$	~$N(0,\sigma_a^2)$
	Centered	$\bar{\phi}_2 = -.5141$	$S_a = 0.134$	The ACF and PACF are well behaved.
	$\bar{Y} = -1.80$	$\bar{\theta}_2 = 0.2972$		
	$S_Y = 0.404$	$\bar{\theta}_3 = 0.3682$		
		$\bar{\theta}_4 = 0.1162$		

*In all three cases the histograms of the residuals of the ARIMA fit indicated normality.

V. SUMMARY

The purpose of this research on the 1980 APG test data was to provide a simulation of the response of the passive and active sensors by time series analysis. Two successful models have been developed. These simulations have provided a realistic method to introduce false alarms and the distortion of target signatures due to the clutter from grassy fields into the study of the performance of various weapon systems. The important findings of this research are presented below.

The millimeter wave radiometric data, collected in July 1980 at APG and analyzed in this report, has resulted in the same ARIMA(1,0,1) structure as the August 1978 radiometric data collected at Rome, New York, with a similar sensor. A plot of (L,Z_t) for $L=1,500$ is shown in Figure 20, where Z_t is generated using Equation (III.4) and the parameter values in Table 8, and then calibrated in Kelvins. If this plot is compared with the actual radiometric data in Figure 1, the agreement is good except for the seasonal variation of the actual data with a period of approximately 300 lags.

There are some possible physical explanations of this cyclic behavior, which were not present in the Rome tests, viz.,

1. In the Rome tests the radiometer was the only sensor being tested, whereas in the 1980 APG tests the radiometer was placed on a spinning mount along with an active sensor. The two sensors shared the same receiving antenna, and there may have been some radar interference with the radiometer.

2. There may have been some problem with the slip rings through which the radiometric signal was carried to the recording devices.

3. There may have been some radio frequency interference, (RFI).

To address the cyclic behavior of the data by time series modeling is a non trivial problem of seasonality, which has not been attempted in this report. Basically, our simulation is felt to be an adequate representation of the original data.

There are some other differences between the Rome tests and the APG tests. Both data sets were digitized at the rate of 2000 samples per second. Since the spin rate of the radiometer was 4 rps at Rome and 3 rps at APG, there were 500 observations per revolution of the sensor at Rome compared with $\approx$ 667 observations per revolution at APG. In each test the helicopter flew at approximately the same speed. This means that the consecutive digitized footprints of the sensor on the ground were closer to each other at APG than at Rome. Therefore, the ACF of the APG data had a stronger autoregressive structure; i.e., the values of the ACF at the various lags were closer to unity for the 36 lags studied than the values of the ACF for the Rome data.

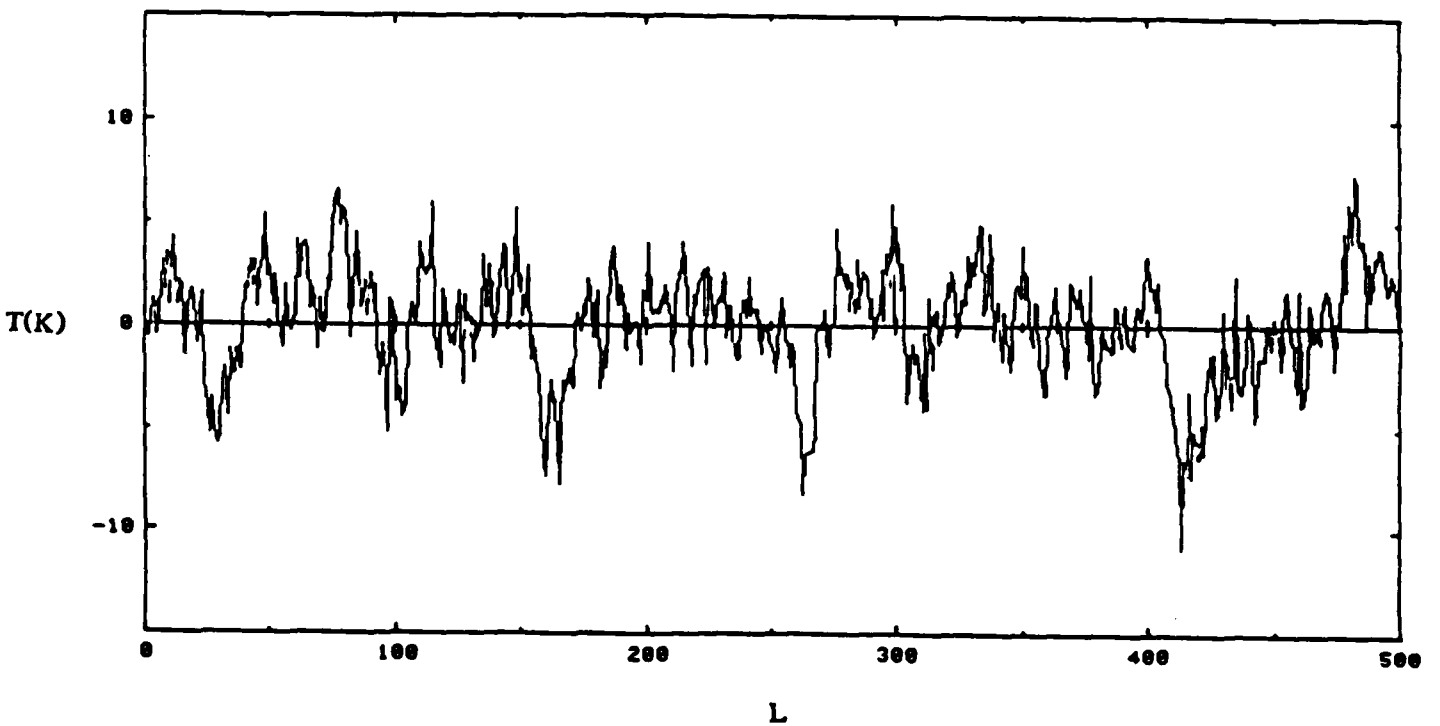

Figure 20 The Simulated Contrast Temperature Data T(K) for a Field at 90m Slant Range is Plotted Against the Integer Number L of Time Steps, ($\Delta t = .5ms$).

Finally, the two tests were not carried out on identical grassy fields, nor were the weather conditions exactly the same. Nevertheless, it is worth noting that the same ARIMA(1,0,1) model adequately describes both the Rome and APG data.

On the other hand the millimeter wave radar data, collected simultaneously with the July 1980 radiometer data at APG and analyzed in this report, at first had to be transformed by a Box-Cox transformation before the time series analysis could be done. The reason for the transformation was that the the original radar data was skewed and the deviations were not symmetric about the mean as well as having positive deviations larger in magnitude than those in the negative direction. In order to balance the positive and negative magnitudes of the deviations, the properties of a log transformation with a shift of -2.91 was used. Then, this transformed data was analyzed using the Box and Jenkins process. The analysis indicated an autoregressive- moving average ARIMA model of order $p=2$ and $q=2,3,4$. A plot of (L,Z_t) for $L=1,500$ is shown in Figure 21, where Z_t is generated using Equations (IV.8) and (IV.9) and the parameter values in Table 12, and then calibrated as radar cross section in meters squared. If this plot is compared with the original data of Figure 2, the agreement is quite satisfactory.

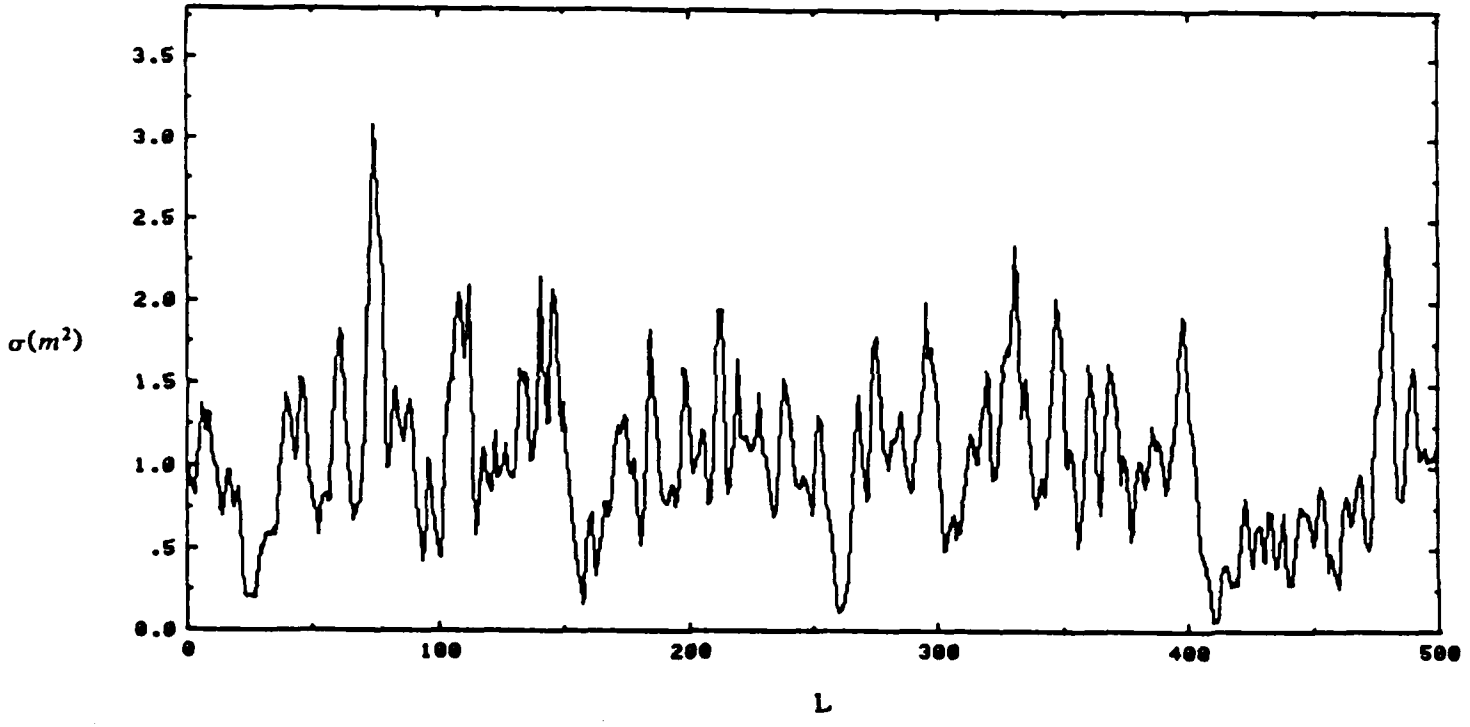

Figure 21 The Simulated Radar Cross Section $\sigma(m^2)$ for a Field at 90m Slant Range is Plotted Against the Integer Number L of Time Steps, ($\Delta t = .5ms$) .

ACKNOWLEDGEMENTS

We wish to express our thanks to Richard Mc Gee, Donald Bauerle, Joseph Knox, H. Bruce Wallace, and Bruce Caudill of the Millimetre-Wave Group at BRL for obtaining the original data, which was analyzed in this report. This group was always helpful in solving the many problems connected with the processing of the data and in explaining its physical significance. We also want to thank Robert Martz and Earl Ball of BRL for the actual digitization of the data. Larry Whiting of the Simulation/Software Division of the HQ TECOM Analysis Directorate deserves credit for providing computer assistance. Finally, we greatly appreciate the scientific direction as well as the continual support for this work which was provided by Robert Gschwind of the Infantry Team in BRL.

REFERENCES

1. Box,G. E. P. and Jenkins, G. M.,"Time Series Analysis: Forcasting and Control", Holden-Day, Inc., San Francisco, Ca., 1970.

2. Maruyama, R. T.,"A Time Series and Intervention Analysis of Millimeter-Wave (MMW) Radiometric Data", ARBRL-TR-02338, July 1981.

3. Lon-Mu Liu,"User's Manual for BMDQ2T(TSPACK) Time Series Analysis (Box-Jenkins)", Technical Report No. 57, Department of Biomathematics, University of California, Los Angeles, 1979.

APPENDIX A

A time series data transformation that is required for the radar data in using the Box-Jenkins modeling approach is as follows:

Data Transformation (Box-Cox)

- Order/ranking of original observations is maintained after the transformation.
- The deviations of the transformed data are symmetric about the mean.

Hence,a natural logarithmic transformation $ln(\bullet)$ was selected, which maintains the order of the original observations. The minimum, mean, maximum, and standard deviation of the random variable $\{Z_t\}$ for the first data set is:

$$\min ln(Z_t) = 1.09 ,$$

$$\text{mean } ln(Z_t) = 1.12 ,$$

$$\max ln(Z_t) = 1.22 ,$$

$$\text{standard deviation of } ln(\bullet) = 0.0223$$

One method of accomplishing symmetry about the mean is by setting the transformation of the original data $\{Z_t\}$ such that the extreme deviations from the mean are equal. That is,

$$[\, ln(\, 3.40 + \Delta\,) - ln(\, 3.08 + \Delta\,)\,] = [\, ln(\, 3.08 + \Delta\,) - ln(\, 2.96 + \Delta\,)\,] \quad \text{(A.1)}$$

where Δ is a shift. Then

$$ln(\, 3.40 + \Delta\,) + ln(\, 2.96 + \Delta\,) = 2\, ln(\, 3.08 + \Delta\,) . \quad \text{(A.2)}$$

If the $ln(\bullet)$ is removed,

$$(\, 3.40 + \Delta\,)(\, 2.96 + \Delta\,) = (\, 3.08 + \Delta\,)^2 , \quad \text{(A.3)}$$

where $\Delta = -2.89$.

Using the $\{\, ln(\, Z_t - 2.89\,)\,\}$ transformation results in

$$\min Y_t = -2.66 ,$$

$$\text{mean } Y_t = -1.73 ,$$

$$\max Y_t = -0.673 ,$$

$$\text{standard deviation} = 0.329$$

$$\Delta_L = \textit{mean } Y_t - \min Y_t = 0.93,$$

and

$$\Delta_M = \max Y_t - \textit{mean } Y_t = 1.057 .$$

Then,

$$\Delta_M - \Delta_L = .127,$$

which implies that the deviation in the maximum (positive direction) is larger by .127. It is desirable to back shift by .5(.127) = .0635 . So an adjustment was made to a shift of -2.91 with the result that

$$\min Y_t = 2.9957 ,$$

$$\text{mean } Y_t = -1.85 ,$$

$$\max Y_t = -0.71335 ,$$

$$\text{standard deviation} = 0.370$$

$$\Delta_L = 1.145 ,$$

and

$$\Delta_M = 1.138 .$$

Hence, the $Y_t = ln(Z_t - 2.91)$ data transformation accomplishes the objective of making the deviation symmetric about is mean.

DISTRIBUTION LIST

No. of Copies	Organization
12	Administrator Defense Technical Info Center ATTN: DTIC-DDA Cameron Station Alexandria, VA 22314
1	Director Defense Advanced Research Projects Agency Tactical Technical Office 1400 Wilson Blvd. Arlington, VA 22209
1	Director Institute for Defense Analysis ATTN: Dr. Bruce J. Whittemore 1801 Beauregard Street Alexandria, VA 22311
1	Deputy Secretary of Defense R&E Tactical Warfare Programs Washington, DC 20310
1	Commander US Army Materiel Development and Readiness Command ATTN: DRCDMD-ST 5001 Eisenhower Avenue Alexandria, VA 22333
2	Commander US Army Armament Research and Development Command ATTN: DRDAR-TSS Dover, NJ 07801
5	Commander US Army Armament Research and Development Command ATTN: DRDAR-LC, Dr. Frasier Mr. P. Granger DRDAR-LCS, Mr. M.J. Brooks DRDAR-LCA, Mr. P. Kisatski DRDAR-TDC, Dr. D. Gyorog Dover, NJ 07801
1	Commander US Army Armament Research and Development Command ATTN: DRDAR-DP, Mr. Chase Dover, NJ 07801
1	Commander US Army Armament Materiel Readiness Command ATTN: DRSAR-LEP-L, Tech Lib Rock Island, IL 61299
1	Commander US Army Aviation Research and Development Command ATTN: DRDAV-E 4300 Goodfellow Blvd. St. Louis, MO 63120
1	Director US Army Air Mobility Research and Development Laboratory Ames Research Center Moffett Field, CA 94035
1	Director Applied Technology Laboratory US Army Research & Technology Laboratories (AVRADCOM) ATTN: DAVDL Fort Eustis, VA 23604
1	Commander US Army Electronics Research and Development Command Technical Support Activity ATTN: DELSD-L Fort Monmouth, NJ 07703
1	Commander US Army Communications Research and Development Command ATTN: DRDCO-PPA-SA Fort Monmouth, NJ 07703

DISTRIBUTION LIST

No. of Copies	Organization
3	Commander US Army Harry Diamond Laboratory ATTN: DELHD-TI ATTN: DELHD-SA, Mr. W. Pepper Mr. J. Salerno 2800 Powder Mill Rd Adelphi, MD 20783
2	Commander US Army Missile Command ATTN: DRSMI-R DRSMI-YDL Redstone Arsenal, AL 35898
3	Commander US Army Missile Command ATTN: DRSMI-CA, Dr. D. McDaniels DRSMI-EA, Mr. B. Harwell DRSMI-RE, Mr. H. Green Redstone Arsenal, AL 35898
1	Commander US Army Missile Command DRSMI-RED, Dr. J. Wright Redstone Arsenal, AL 35898
1	Director Office of Missile Electronic Warfare ATTN: DRSEL-WLH-SF, Mr. R.J. Clawson White Sands Missile Range, NM 88002
1	Commander US Army Night Vision and Electro-Optics Laboratory ATTN: DRSEL-NV-VI, Mr. J. Dehne Fort Belvoir, VA 22060
1	Commander US Army Mobility Equipment Research & Development Cmd ATTN: DRDME-ZK, Dr. Steinbach Fort Belvoir, VA 22060
1	Commander US Army Tank Automotive Research & Development Cmd ATTN: DRDTA-UL Warren, MI 48090
1	Commander US Army Training and Doctrine Command ATTN: ATCG, Dr. Marvin Pastel Fort Monroe, VA 23651
1	Commander Studies and Analysis Directorate, Methodology Br ATTN: DCSCO, Mr. R.T. Maruyama Fort Monroe, VA 23651
1	Director US Army TRADOC Systems Analysis Activity ATTN: ATAA-SL, Tech Library White Sands Missile Range, NM 88002
1	Commander US Army Infantry Center ATTN: ATSH-DCG Fort Benning, GA 31905
1	Commandant US Army Armor School ATTN: Combat Developments Fort Knox, KY 40121
3	Commander US Army Waterways Experiment Station Corps of Engineers ATTN: Mr. Wade West Mr. Robert Benn Mr. Jerry Lundien P.O. Box 631 Vicksburg, MS 39181
1	Director US Army Armament Research and Development Command ATTN: DRDAR-LCB-TL Watervliet, NY 12189

DISTRIBUTION LIST

No. of Copies	Organization
1	ADTC/DLMIT Eglin AFB, FL 32542
1	AFATL (Dr. J.R. Mayersak, Chief Scientist) Eglin AFB, FL 32542
1	AFELM, The Rand Corporation ATTN: Library-D 1700 Main Street Santa Monica, CA 90406
1	Aerojet Electro Systems ATTN: Mr. Keith Paradis 1100 W. Hollyvale Street Azusa, CA 91702
1	Applied Electronics Division AIL - Division of Cutler-Hammer ATTN: Mr. Theodore Flattau Melville, LI, NY 11746
1	AVCO Systems Division ATTN: Mr. Thomas Midura 201 Lowell Street Wilmington, MA 01887
2	Cincinnati Electronics ATTN: Mr. Robert Seitz Mr. Raymond Schmidt 2630 Glendale-Milford Road Cincinnati, OH 42541
1	General Dynamics Pomona Division ATTN: Mr. L.P. Green P.O. Box 2507 Pomona, CA 91766
2	Honeywell, Inc. ATTN: Mr. David P. Erdmann Mr. E. Brindley 600 Second Street, North Hopkins, MN 55343
2	Hughes Aircraft Company Ground Systems Group ATTN: Dr. Wesely K. Masenten Mr. J. Willner P.O. Box 3310 Fullerton, CA 92631
1	Hughes Aircraft Company ATTN: Mr. Ron Sabowski 3100 W. Lomita Blvd Torrance, CA 90509
1	Martin Marietta Corporation Orlando Division ATTN: Mr. Joseph Stever P.O. Box 5837 Orlando, FL 32805
1	Systems Planning Corp. ATTN: Dr. James Meni 1500 Wilson Blvd Suite 1500 Arlington, VA 22209
2	Singer-Kearfott Division ATTN: Mr. John Brinkman Mr. Robert Slater 150 Totwa Road Wayne, NJ 07470
1	University of Wisconsin Dept. of Mathematics ATTN: Dr. G. E. P. Box 1225 W. Dayton St. Madison, WI 53706
1	University of California Lawrence Livermore National Laboratory ATTN: Dr. William J. Singleton, L-9 P.O. Box 808 Livermore, CA 94550

DISTRIBUTION LIST

Aberdeen Proving Ground

Dir, USAMSAA
ATTN: DRXSY-D
DRXSY-MP, Mr. H. Cohen
DRXSY-DS, Mr. J. Kramar
Mr. J. Chernick

Dir, HEL
ATTN: Mr. D. Giordano

CDR, USATECOM
ATTN: DRSTE-TO-F

Dir, USACSL
Bldg E3516, EA
ATTN: DRDAR-CLB-PA

USER EVALUATION OF REPORT

Please take a few minutes to answer the questions below; tear out this sheet, fold as indicated, staple or tape closed, and place in the mail. Your comments will provide us with information for improving future reports.

1. BRL Report Number_____

2. Does this report satisfy a need? (Comment on purpose, related project, or other area of interest for which report will be used.)

_____

_____

_____

3. How, specifically, is the report being used? (Information source, design data or procedure, management procedure, source of ideas, etc.)_____

_____

_____

4. Has the information in this report led to any quantitative savings as far as man-hours/contract dollars saved, operating costs avoided, efficiencies achieved, etc.? If so, please elaborate.

_____

_____

5. General Comments (Indicate what you think should be changed to make this report and future reports of this type more responsive to your needs, more usable, improve readability, etc.)_____

_____

_____

_____

6. If you would like to be contacted by the personnel who prepared this report to raise specific questions or discuss the topic, please fill in the following information.

Name:_____

Telephone Number:_____

Organization Address:_____

_____

_____

FOLD HERE

Director
US Army Ballistic Research Laboratory
Aberdeen Proving Ground, MD 21005

NO POSTAGE
NECESSARY
IF MAILED
IN THE
UNITED STATES

OFFICIAL BUSINESS
PENALTY FOR PRIVATE USE, $300

BUSINESS REPLY MAIL
FIRST CLASS PERMIT NO 12062 WASHINGTON, DC
POSTAGE WILL BE PAID BY DEPARTMENT OF THE ARMY

Director
US Army Ballistic Research Laboratory
ATTN: DRDAR-TSB -S
Aberdeen Proving Ground, MD 21005

FOLD HERE